TECHNICAL PROGRESS REVIEW

REACTOR CORE MATERIALS

Prepared for U. S. ATOMIC ENERGY COMMISSION by the BATTELLE MEMORIAL INSTITUTE

MAY 1958 VOLUME 1 NUMBER 2

TECHNICAL PROGRESS REVIEWS

To meet the needs of industry for concise summaries of current atomic developments, the AEC is publishing this series, Technical Progress Reviews. Issued quarterly, each of the reviews digests and evaluates the latest findings in a specific area of nuclear technology and science.

The three journals currently published in this series are:

Power Reactor Technology, Walter H. Zinn and associates, General Nuclear Engineering Corporation

Reactor Fuel Processing, Stephen Lawroski and associates, Chemical Engineering Division, Argonne National Laboratory

Reactor Core Materials (covering solid material developments), R. W. Dayton, E. M. Simons, and associates, Battelle Memorial Institute

Each journal may be purchased by subscription (domestic, $2.00 a year; foreign, $2.50 a year) or by individual issue (55¢) from the Superintendent of Documents, U. S. Government Printing Office, Washington 25, D. C.

●

Availability of Reports Cited in This Review

Unclassified AEC reports are available for inspection at AEC depository libraries and are sold by the Office of Technical Services, Department of Commerce, Washington 25, D. C.

Unclassified reports issued by other Government agencies or private organizations should be requested from the originator.

Unclassified British and Canadian reports may be inspected at AEC depository libraries. British reports are sold by the British Information Service, 30 Rockefeller Plaza, New York, N. Y.; Canadian reports (AECL series) are sold by the Scientific Document Distribution Office, Atomic Energy of Canada, Ltd., Chalk River, Ontario, Canada.

Classified U. S. and foreign reports identified in this journal as Secret or Confidential may be purchased by properly cleared Access Permit Holders from the Technical Information Service Extension, U. S. Atomic Energy Commission, P. O. Box 1001, Oak Ridge, Tenn. Such reports may be inspected at classified AEC depository libraries.

REACTOR CORE MATERIALS

a review of recent developments in solid materials for reactor cores

prepared by
BATTELLE MEMORIAL INSTITUTE

MAY 1958 VOLUME 1 NUMBER 2

foreword

This is the second of a series of quarterly publications covering significant developments in the field of solid reactor core materials. Like the first, it is a compilation of reviews of specialized topics prepared by staff members of Battelle Memorial Institute at the request of the Division of Information Services of the U. S. Atomic Energy Commission.

The purpose of this review series is to provide a convenient condensed source of information to two types of readers: (1) those who wish to keep abreast of developments in a general way and (2) those interested in learning where to find detailed accounts of work in particular areas. Complete bibliographies are provided at the end of each section for the benefit of the latter. Coverage has been limited to those core materials which are solid at reactor operating temperatures.

In writing this report the authors have concentrated on recent significant advances and new concepts with good promise. Wherever possible, developments in different laboratories along similar lines have been brought together into correlated reviews.

To improve readability, this issue has been organized somewhat differently from the first. One change is the addition of a separate section to treat cladding and structural materials. Further, two sections in the first report, corrosion and radiation effects, have been eliminated and information in these subject areas incorporated in other sections of the Review where particular materials are discussed.

R. W. DAYTON
E. M. SIMONS
Battelle Memorial Institute

contents

ii		Foreword
1	I	Fuel and Fertile Materials
20	II	Moderator Materials
24	III	Control Materials
28	IV	Cladding and Structural Materials
39	V	Special Fabrication Techniques

Issued quarterly by the U. S. Atomic Energy Commission. Use of funds for printing this publication approved by the Director of the Bureau of the Budget on November 1, 1957.

SUBSCRIPTIONS

REACTOR CORE MATERIALS is available on subscription for $2.00 per year domestic, $2.50 foreign, 55 cents per copy, through the Superintendent of Documents, U. S. Government Printing Office, Washington 25, D. C.

Unalloyed Uranium

Heat-Treatment and Irradiation Studies

Du Pont, in studies involving the beta transformation of uranium,[1] found that the rate of loss of preferred orientation during heat-treatment at low beta-phase temperatures was markedly less than the rate of coarsening of grains. To explain the difference, it was postulated that halting the transformation at an intermediate stage by cooling leaves residual alpha-phase metal to act as nucleation centers for the regrowth of an oriented but large-grained structure. Intermediate size grains were produced by halting the transformation of small-grained metal at an early stage. A similar interruption of the transformation of initially large-grained metal did not result in a significant refinement of grain size.

Results of a recent investigation at Hanford[2] suggest that, on rapid cooling, uranium undergoes a martensitic beta-to-alpha transformation. These results support other documented evidence. Many of the arguments opposing such a mechanism stem from assuming a shear hypothesis for martensitic transformation, which permits no depression of the transformation point by increased cooling rates, and from the nature of the transformation during slow cooling where diffusion would be expected to predominate.

Further difficulty in understanding the true nature of the beta-to-alpha transformation arises from the complexity of grain formation. Grain growth might occur by a combination of diffusion and nondiffusion mechanisms to satisfy valence-bonding and close-packing requirements of the atoms simultaneously. It has been suggested that subgraining, prominent in alpha grains, results from combined polygonization and nuclei rotation. As a result uranium cooled at moderate rates through the transformation point should exhibit less distortion and more subgraining due to polygonization than uranium cooled at much faster rates.

It is significant that a wide range of structures with varying grain size, symmetry, and deformation can be obtained by controlling the cooling rate through the beta-to-alpha transformation. Further knowledge of the effects of these variants on the mechanical properties of uranium are required before optimum heat-treatments can be specified.

Since thermal cycling and irradiation behavior and the fabrication characteristics of unalloyed uranium are strongly dependent on grain size, the current interest in the use of as-cast fuel material has been responsible for several sites investigating the effectiveness of heat-treatment as a means of refining as-cast structures. One of these studies, performed at Nuclear Metals, Inc.,[3] resulted in the following conclusions being drawn.

1. The grain size of cast uranium may be refined appreciably by beta quenching.
2. Time and temperature in the beta phase are not critical in determining the final alpha grain size.
3. Multiple beta quenches (two to four times) produce better grain refinement than a single quench.
4. Alpha annealing after beta quenching causes recrystallization but does not greatly affect the grain size.
5. Gamma quenching is not recommended as a practical heat-treatment.

Additional work at National Lead Co. on centrifugally cast metal confined itself to the beta heat-treatment.[4] The results confirmed the increased grain refinement of multiple quenches and also indicated that the magnitude of grain-size changes (some coarsening was observed)

depended on level of impurity content. Iron and manganese were cited. A tabulation of the effects noted is shown below:

Impurity	Concentration, ppm	Effect noted
Iron	0–40	Significant refinement
	41–100	Little refinement
	>100	No significant refinement
Manganese	0–20	Significant refinement
	>20	Grain coarsening indicated

Argonne[5] has performed experiments on the effects of high burn-up of natural uranium. The metal was irradiated to 1.82 at.% (15,500 Mwd/ton) burn-up at temperatures from 50 to 220°C. Specimens had four different fabrication histories:

1. Rolled at 300°C
2. Rolled at 300°C, quenched from beta phase
3. Rolled at 300°C, quenched from the beta phase, and recrystallized in the alpha phase
4. Rolled at 600°C

Samples of Group 1 grew at a rapid rate (under irradiation), although they maintained relatively smooth surfaces. The growth rate appeared to decrease with increasing irradiation temperature. Group 2 specimens were more stable dimensionally but developed roughened surfaces. Group 4 samples showed intermediate behavior. Specimens of Group 3, it was concluded, can withstand at least 2 at.% burn-up without disintegration due to radiation damage.

English investigators[6] have studied the effects of heat and pressure on the swelling of irradiated uranium. Small pieces of uranium bar which had been irradiated to 0.3 to 0.4 at.% burn-up were heat-treated either *in vacuo* or at high pressures, and changes in their density were measured. On heating *in vacuo* the volume was found to increase initially by about 2 per cent at 575°C and about 5 per cent at 810°C. The swelling increased to as much as 15 per cent with various cycling treatments *in vacuo* but was reduced by subsequent annealing under pressure. Examination of the microstructure of the swollen metal showed gas collected in voids less than 2000 A in diameter and some cracks, their total volume being sufficient to account for the swelling. The majority of the volume increase is attributed to the smaller bubbles. The initial swelling was found to be due to this formation of bubbles of fission gas within the uranium; the presence of irradiation, other than to produce the rare gases by fission, is not essential for swelling to occur. This work is discussed in more detail on pp. 16–17.

Results of an investigation of the effect of irradiation on unalloyed uranium indicate that for burn-ups to 0.10 wt.% most of the changes in room-temperature mechanical properties occur in the first 0.02 wt.% burn-up (Fig. 1). This work also has shown that annealing above 760°C will produce recovery of elongation of irradiated uranium with 0.07 and 0.10 at.% burn-up. Recovery was also observed in low burn-up specimens annealed in the alpha range.

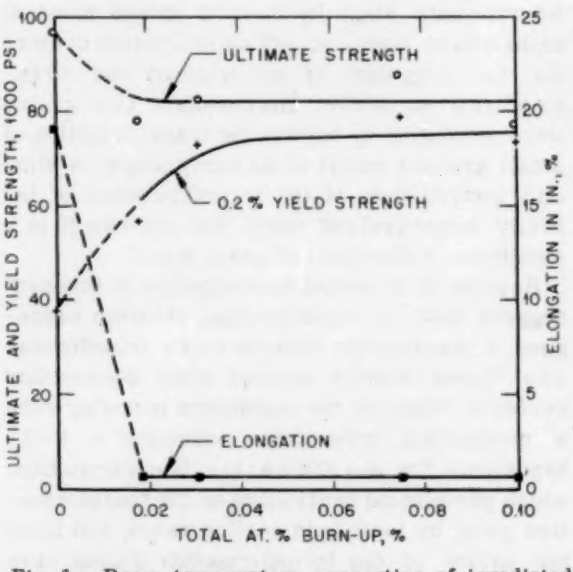

Fig. 1—Room-temperature properties of irradiated uranium; effect of exposure.

This is the first observed recovery in irradiated uranium. Pre- and postirradiation metallographic examinations of the same areas have been partially completed on uranium specimens irradiated to 0.03 and 0.07 at.% burn-up. The type and degree of damage varied from little or none to broadening of twins, grain-boundary agglomeration, and formation of microcracks. Fractographs of a broken irradiated-uranium tensile specimen showed that the specimen had

a surface similar to that observed in unirradiated impact specimens broken at −200°C.

(M. S. Farkas)

Corrosion Mechanisms

The reaction of superheated steam at atmospheric pressure with unalloyed uranium at temperatures ranging from 160 to 1400°C has been studied by a thermogravimetric method at Harwell.[7] Up to 880°C the reaction was found to follow a linear rate law, with maximum rates of 2.7 and 6 mg/(cm^2)(min) at 300 and 750°C, respectively. Above 880°C a parabolic rate law applied for the first 60 to 120 min, after which the corrosion rate became constant at about 0.2 to 0.3 mg/(cm^2)(min), corresponding to the rates at about 200°C. After testing, uranium hydride was observed at grain boundaries in the specimens subjected to the latter treatment.

Linear rates at temperatures below 450°C were explained on the basis of the generally accepted theory that the intermediate production of a reactive hydride in the corrosion process is unlikely to lead to the formation of a protective film. Above 450°C the formation of hydride is improbable. The high rates observed in the 450 to 880°C range were believed to be a result of the surface area increasing during corrosion. Above 880°C it was believed that a protective oxide film formed during the initial period. Stresses in the oxide film caused cracking when it reached a certain critical thickness. The oxide layer adjacent to the metal remained intact, but the outer layer became nonprotective. The rate was then controlled by diffusion through an oxide layer of fixed thickness. This explained the initial parabolic rate followed by a linear rate.

The diffusing species was believed to be hydroxyl ions from a chemisorbed complex of water vapor formed on the uranium oxide at the steam-oxide interface. The hydroxyl ions, rather than oxygen ions, then diffused through the oxide film to the uranium oxide interface. There the hydroxyl ions reacted with uranium to form more oxide and liberate hydrogen. Some of the hydrogen then dissolved in the gamma uranium. When the specimen was cooled to room temperature, the hydrogen solubility in the alpha uranium was exceeded and hydrides precipitated out at the grain boundaries.

(W. E. Berry and A. W. Lemmon, Jr.)

Alpha-Uranium Alloys

A Chalk River[8] loop test on defected diffusion-annealed Zircaloy-2 coextrusion-clad specimens of a uranium−2 wt.% zirconium alloy has been completed. The object of the test was to determine if a defected specimen could be detected soon enough to allow time for reactor shutdown before catastrophic failure. Conclusions were reached by testing the above-mentioned specimen. The diffusion anneal was performed at 800°C for 24 hr, followed by furnace cooling; the interfacial diffusion layer varied from 0.002 to 0.005 in. The clad was then defected with a 0.020-in.-diameter hole. Irradiation took place at 500°F.

Results of the test show the following:

1. Corrosion of the uranium will occur, and a compact layer of uranium oxide will be formed at the base of the defect. As the corrosion process continues, the accumulated oxide will force the clad into a small pimple. This may take 1 or 2 hr, or many hours, depending on the strength of the cladding. During this time, the presence of the oxide undoubtedly hampers the access of the water to the metal, and the corrosion rate is determined by the rate water can diffuse through the compact oxide.

During this time, no detectable fission products are released to the circulating water, and hence there is no way of telling a cladding failure has occurred.

2. After a certain time the pimple will rupture, releasing accumulated oxide and fission products to the water and giving a sharply rising signal on monitors in the stream. The rupture may be brought about by thermal cycling. After the rupture, water has free access to the core metal and rapid corrosion will occur.

3. If, from the time the signal is received, the circulating water is cooled to a temperature below 300°F in less than 30 min, no extensive damage will have resulted, and the fuel element may be removed from the loop or reactor. Argonne[9] reports that 1 at.% burn-up apparently does not affect the protective action of the diffusion barrier.

Aqueous corrosion tests on uranium−5 wt.% zirconium−2 wt.% tantalum were performed at Argonne.[9] The alloy was tested after various heat-treatments and after rolling. It was found that, in general, the alloy is not corrosion resistant. The corrosion behavior of quenched

and of quenched and aged alloys is presented in Table I-1. It is suspected that the alloys were inhomogeneous.

Constitution studies are being performed by the British[10] and Argonne[9] on the high-uranium

Table I-1 AQUEOUS CORROSION OF URANIUM–5 WT.% ZIRCONIUM–2 WT.% TANTALUM AT 290°C (ARGONNE DATA[9])

Test interval, days	Average rate of weight loss, mg/(cm²)(day)	
	Quenched from 1070°C	Quenched and aged at 400°C–1 hr
3.75	16.1	14.1
6.0	31.6	230

end of the uranium-ruthenium phase diagram. Some observations from this work are:

1. The solidus and liquidus of the uranium-rich uranium-ruthenium alloys are depressed 5 and 1°C, respectively, for 1 at.% ruthenium addition.[10]

2. A eutectic occurs[10] at 900°C and 18 at.% ruthenium, between uranium and an intermetallic compound (U_2Ru).

3. The alpha-to-beta and beta-to-gamma transformation temperatures are lowered by ruthenium.[10]

4. The solubility of ruthenium in gamma uranium is approximately 10 at.% at 900°C, the solubility in alpha being considerably lower.[10]

5. Gamma is retained on quenching a uranium–5 wt.% ruthenium alloy, the lattice parameter[9] being 3.46 A.

6. The beta-to-gamma transformation temperature[9] is reported as 708 ± 2°C.

7. The gamma-to-liquid transformation takes place[9] at 898 ± 2°C.

Several recently published papers and monographs covering the field of alpha-uranium alloys[11–13] are worthy of attention by readers having a general interest in the background technology. (M. S. Farkas)

Gamma-phase Uranium Alloys

In connection with the beneficial effects of zirconium in uranium-niobium alloys, Argonne[14] has issued a report of studies of the constitution of the uranium-rich portion of the uranium-niobium and uranium-niobium-zirconium systems. The ternary system is of particular interest since it is found that the miscibility gaps in the binary systems close with the addition of the third element and that the addition of both zirconium and niobium stabilizes the body-centered-cubic gamma phase to lower temperatures than in the binaries. It is also reported that the gamma phase can be retained in alloys richer in composition that those between the uranium–6 wt.% niobium and uranium–25 wt.% zirconium compositions.

Ames[15] is engaged in bomb-reduction studies of the preparation of uranium-niobium alloys by coreduction of UF_4 and Na_2NbOF_5 with calcium. Contaminant analyses have been erratic, but nitrogen and carbon contents have been found to exceed allowable limits of 200 ppm.

Uranium-Molybdenum Alloys

A summary of irradiation and corrosion behavior of bare uranium alloys containing 9 to 15 wt.% molybdenum has been issued by the Naval Reactors Branch.[16] Uranium-molybdenum alloys have shown excellent dimensional stability, although irradiation temperatures were not carried beyond 800°F and burn-ups were limited to 0.5 at.%.

A summary report of irradiation data has been prepared by Bettis.[17] Volume changes accompanying irradiation are summarized in Fig. 2. Maximum density decreases of 4.4 per cent at an exposure of 8800 Mwd/ton at temperatures below 428°C in bare specimens, and of 4.3 per cent at 28,200 Mwd/ton at core temperatures to 654°C in the clad specimens, were noted. Splitting accompanied the latter density changes, and no significant effect of temperature was noted.

Bettis also reports[17] that density, hardness, and electrical-resistivity changes in irradiated alpha-transformed uranium-molybdenum alloys indicated radiation-induced reversion to the gamma phase. Hardness and electrical-resistivity changes in gamma-quenched samples approached a saturation limit. A maximum hardness change of 90 DPH was noted after an exposure of 8000 Mwd/ton.

Room-temperature bend tests of irradiated gamma-quenched 10.5 and 12 wt.% molybdenum samples indicated sharply reduced ductility after an exposure of 700 Mwd/ton. However, molybdenum appears to improve resistance to radiation-induced embrittlement, complete embrittlement of unalloyed uranium resulting at exposures as low as 65 Mwd/ton.

Radiation produced no significant changes in corrosion rates of gamma-quenched uranium-molybdenum alloys in 650°F water. However, the failure time for unclad specimens was reduced, uranium–12 wt.% molybdenum samples irradiated to a maximum exposure of 2000 Mwd/ton disintegrating in 650°F water in one to seven days as compared with 66 days for unirradiated control specimens. Clad samples

Bettis also reports[18] that graphite molds can be employed to cast successfully the uranium–12 wt.% molybdenum alloy in shapes approximately 2 in. in diameter and 26 in. long while maintaining alloy homogeneity to ±0.3 wt.%. The density of the cast alloy is increased, by consumable-electrode arc melting, by about 0.05 g/cm³ above the average of 16.88 for the induction-cast material.

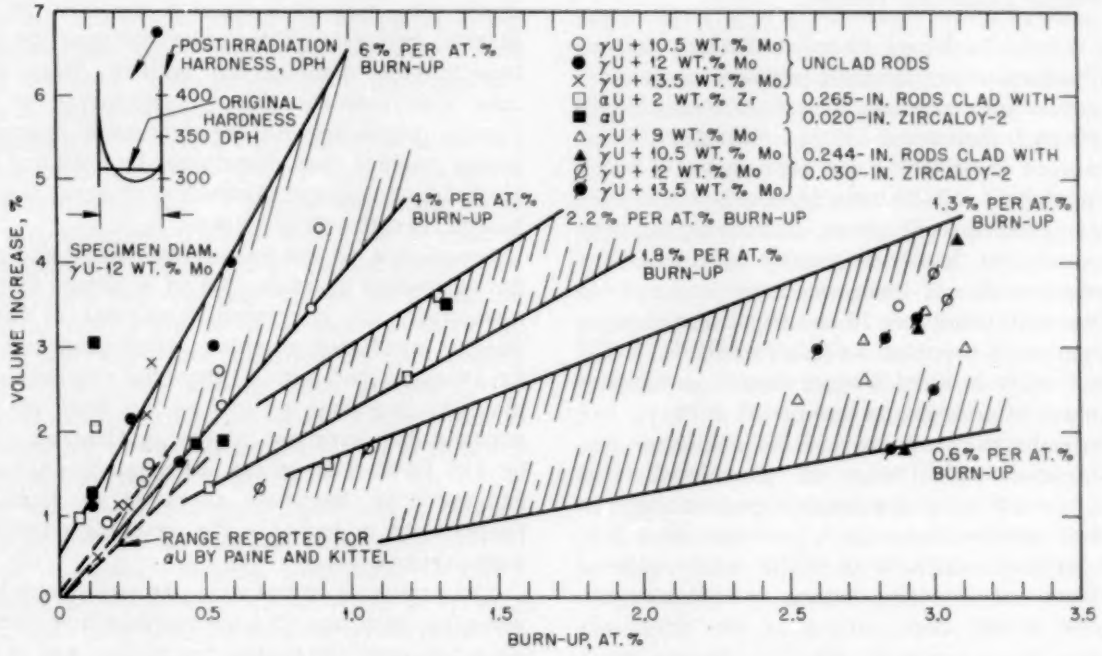

Fig. 2—Volume changes as a result of irradiation. Compiled by Bettis.[17]

irradiated to exposures of approximately 5000 Mwd/ton, defected and corrosion tested, showed no change in corrosion life. In-pile corrosion-tested clad and defected samples withstood exposures to 4000 Mwd/ton in hot-water loops.

Harwell has also studied uranium-molybdenum alloy corrosion employing 4, 7, and 13 wt.% molybdenum alloys. Failure in 300°C (570°F) water by cracking and crumbling was observed in these alloys, with hydride formation apparently being responsible for the disintegration. This observation parallels other reported observations of failure by hydride formation in these alloys. Increasing the molybdenum content increased the corrosion resistance, but failure still occurred in 30 to 40 days at 300°C in the 13 wt.% alloy, although the initial rate of corrosion was low.

A bibliography of reports concerned with the uranium-molybdenum program has been issued.[19]

Ternary Alloys

Corrosion results on bare uranium–23.8 wt.% zirconium–6.1 wt.% niobium and 23.2 wt.% zirconium–4.8 wt.% niobium alloys in 680°F water are reported by Battelle.[20] After 1515 hr the first alloy is corroding at a rate of 0.04 mg/(cm²)(hr) in the quenched and 500°C aged condition of heat-treatment, whereas specimens of the latter alloy are corroding at rates varying from 0.10 to 0.28 mg/(cm²)(hr), depending on heat-treatment. It appears that the niobium additions stabilized the uranium-zirconium gamma phase.

Preliminary 500°F water-corrosion test results from a study of ternary and quaternary gamma-phase alloys containing niobium, zirconium, molybdenum, ruthenium, vanadium, and chromium additions are also reported.[20]

(A. A. Bauer)

Epsilon-phase Uranium Alloys

Uranium-Zirconium Alloys

A report by Naval Reactors Branch personnel[16] summarizes uranium-zirconium alloy irradiation and corrosion behavior. Uranium–40 to 60 wt.% zirconium alloys irradiated at temperatures up to 700°F and burn-ups of 0.5 at.% have shown satisfactory irradiation and corrosion behavior. However, increasing the uranium content leads to greatly impaired corrosion resistance. This conclusion is supported by Harwell, uranium–30 and 40 wt.% zirconium alloys being reported to fail rapidly in 300°C water while a 50 wt.% alloy showed no signs of cracking after being on test for 35 days.

Battelle has reported on the corrosion behavior in 680°F water of Zircaloy-2–clad uranium–50 wt.% zirconium elements with artificial defects. Specimens survived more than 588 days of exposure in 680°F water with no evidence of bondline attack or catastrophic failure of the core. Attack of the core was dependent on corrosion rate of the bare alloy.

Sylvania has studied hydrided uranium–50 wt.% zirconium epsilon-phase samples by X ray and metallographic means. It appears that hydrogen converts epsilon to a mixture of zirconium hydride and uranium or uranium hydride.[21]

Battelle, in studying the constitution of the uranium-zirconium-titanium system, finds that U_2Ti and epsilon exist together in equilibrium at temperatures below 560°C.

Uranium-Silicon Alloys

The corrosion and irradiation behavior of the uranium-silicon epsilon-phase alloy is summarized in Bettis[17] and Naval Reactors Branch[16] reports. Samples irradiated bare have exhibited density decreases of almost 4 per cent after exposures slightly in excess of 100 Mwd/ton, with little additional density decrease accompanying exposures to 1100 Mwd/ton. The dimensional instability of U_3Si is characterized by bending, cracking, and blistering of fuel samples. The instability is probably related to inhomogeneity of the alloy specimens.

The density decrease observed is believed to occur by disordering of the epsilon phase. This view is supported by resistivity changes measured, the resistivity increasing markedly and exhibiting a negative temperature coefficient typical of gamma-phase alloys. X-ray diffraction data show that a marked reduction in crystallite size accompanies exposure to radiation, rendering the crystal pattern too diffuse to yield a diffraction pattern. These data may also indicate that a disordering of the epsilon phase has occurred since a specimen whose surface was disordered by abrading exhibited a consequent diminution of peak intensities in its diffraction pattern.

Irradiation to low exposures caused samples of epsilonized uranium–3.8 wt.% silicon to lose essentially all corrosion resistance to 650°F water; irradiated samples disintegrated in 22 hr as compared with 84 days for control samples. An exposure as low as 105 Mwd/ton increased the hardness of the epsilonized alloy by 215 DPH. The stress accumulation accompanying this hardness increase is probably responsible in part for the cracking observed under irradiation.

The problems of preparing homogeneous U_3Si samples with the precise composition necessary for good corrosion resistance and of the interaction of U_3Si with Zircaloy during cladding have been studied at Nuclear Metals.[22,23] Little success in eliminating these drawbacks is indicated. Whether the effects of antimony and bismuth in broadening the epsilon-phase region are beneficial is questionable since chemical analyses for silicon were uncertain.

(A. A. Bauer)

Dilute Uranium Alloys

Aluminum-Uranium Alloys

The centrifugal-casting technique appears promising as a method for the production of sound, homogeneous aluminum-uranium alloy extrusion billets. Battelle[20,24] has found that this technique produces sound metal; however, surface condition of the casting is dependent on pouring temperature and speed of mold rotation. To date, a speed of 975 rpm has produced the best results. Variations in uranium

content may exist from end to end in the castings produced. This is a function of the metal distribution system, and several techniques of improving this distribution are being investigated.

Alloys containing 16, 30, and 40 wt.% uranium have been successfully coextruded by Nuclear Metals.[25] Cladding of magnesium-aluminum alloy (outer clad 3 wt.% magnesium, inner clad 5 wt.% magnesium) has been used with the aluminum–35 wt.% uranium alloy. The tube surfaces and the bond appeared good; however, the taper defect at the core-to-end seal interface was longer than that obtained with the aluminum clad.

Battelle[20,24] reports that additions of silicon in amounts up to 1 wt.% have little or no effect on the liquidus line of alloys containing up to 45 wt.% uranium. This is also true of magnesium in the range of 0.5 wt.%. Oak Ridge[26] has determined that soaking the 48 wt.% uranium alloy at 600°C for 50 hr or more weakens the alloy and does not improve the hot-rolling properties. After a 4-hr soak at 600°C, the eutectic UAl_4 is almost completely spheroidized. Treatments of slightly longer than 4 hr resulted in complete spheroidization.

In view of the possibility of using ternary aluminum-uranium-thorium alloys as liquid fuel in U^{233} breeder reactors, Iowa State College[27] studied the aluminum-rich corner of the ternary diagram. Data indicate that the ternary eutectic valleys of the aluminum-uranium and aluminum-thorium systems meet in the neighborhood of 76 wt.% aluminum, 18 wt.% thorium, and 6 wt.% uranium. The solidification temperature of this ternary eutectic is 630°C. There also seems to be a rather wide range of compositions of uranium and thorium in aluminum, varying from 13 wt.% uranium at zero wt.% thorium to zero wt.% uranium at 25 wt.% thorium, that can be maintained as a one-phase liquid solution at temperatures lower than 640°C.

Zirconium-Uranium Alloys

Bettis has reviewed the irradiation data available on uranium-zirconium and reached some interesting conclusions. A study of Knolls data on alloys containing between 7 and 40 wt.% uranium at temperatures between 380 and 690°C and at burn-ups between 0.7 and 4.5 at.% indicates that, below 600°C, the volume change is that which would be expected from normal accommodation of fission products (2 to 3 per cent). This is the case whether the temperature is cyclic or constant. Above 600°C the volume increase is about five times normal at constant temperature and about 20 times normal under cyclic conditions. These specimens exhibit microporosity and cracking at the center.

The 22 wt.% uranium alloys irradiated by Battelle indicate that heat-treatment had no effect on the irradiation stability. These irradiations were at center temperatures of about 400°C and at burn-ups of approximately 1 at.%. Little or no change was noted in the specimens after the irradiation. It is theorized that if many interphase interfaces were present these would provide for nucleation of gas bubbles which should be distributed uniformly throughout the specimen. The 7 wt.% uranium alloys do not seem to show as great an irradiation-induced volume increase as the alloys of higher uranium content. The data reported indicate that there may be a critical temperature above which excessive swelling occurs. Below this temperature lattice accommodation and possible formation of gas bubbles are constrained by metal matrix. Above this temperature the metal yields, permitting expansion.

Knolls reports that after a burn-up of 1.67 at.% five specimens of a zirconium–7 wt.% uranium alloy, Zircaloy-3 clad, exhibited excessively heavy crud deposits on the cladding and about twice the volume and length changes experienced in previous tests under similar burn-ups. Temperature checks were run, and it was determined that maximum core temperature was on the order of 923°F. This would account for the crud and growth. The tests did indicate that the fuel element will perform satisfactorily under design operating conditions. During static irradiations in NaK, 5 of 14 zirconium–7 wt.% uranium reference pins exhibited cladding cracks after burn-ups in the 1 to 2 at.% range. Since the behavior of cladding in similar specimens irradiated under dynamic conditions is generally satisfactory, it is theorized that the NaK may be responsible for the cracking of the clad. This is being investigated.

Bettis reports that Zircaloy-3–clad alloys of 5.5 wt.% uranium, containing 0.06 to 0.113 wt.% boron, exhibit volume changes between 2 to 3 per cent per at.% burn-up. These specimens received burn-ups of 1.58 and 1.76 at.% at temperatures from 190 to 372°F. Another specimen of the alloy was irradiated to a burn-

up of 2.74 at.% at 320°F and underwent a volume change of between 5.4 and 6.4 per cent per at.% (temperatures and burn-ups reported were calculated). Combustion Engineering is irradiating Zircaloy-2–clad alloys containing 8 and 12 wt.% uranium in NaK-filled capsules. These capsules have been charged into the Materials Testing Reactor (MTR), and tests are now in progress on the nonirradiated control samples.

As a result of experiments designed to test the effect of irradiation on fuel-element properties, Knolls reports initial data which indicate that, at least in the case of the 12 wt.% uranium alloy, hydrogen content increases with increase of irradiation time in water. Small amounts of NaCl in water do not affect the corrosion resistance of the fuel alloy. It would, therefore, appear that small amounts of sea water might be tolerated. These tests also show that exposure to NaK prior to water corrosion changes the corrosion behavior in water.

A study of both 7 and 8 wt.% uranium alloys irradiated at a number of burn-ups and given a postirradiation anneal shows that physical changes in the material as a result of the anneal become more gross when the material has received more than 1 at.% burn-up. Bettis[28] reports alloys containing 6, 8, 10, and 12 wt.% uranium were irradiated, both clad and unclad, in NaK capsules to a maximum burn-up of 40 per cent of the U^{235} atoms. There were no major changes in the clad samples; however, the unclad samples were badly warped and the dimensions changed considerably.

Fuel elements containing zirconium–12 wt.% uranium alloy clad with Zircaloy-3 were tested by Knolls in a loop and were subjected to an equivalent full-power flux for 6860 hr (burn-up 2.4 at.%). There was no detectable cracking before decrudding, and little or no wear was noted. These elements will be examined further. (R. F. Dickerson)

Plutonium Alloys

Unalloyed Plutonium

Zone refinement is being studied as a method of purification of plutonium at Los Alamos.[29] The reported procedure was to pass an induction coil along an extruded rod 0.25 in. in diameter by 6 in. long contained in a thoria boat under vacuum. Passing the coil along the rod at 0.5 in./hr was more effective than 1.3 in./hr, giving considerable cleanup of inclusions. Based on these tests, the process appears capable of lowering the amount several impurities including silicon, iron, nickel, chromium, manganese, and perhaps others.

Plutonium-Aluminum

Research on aluminum-rich alloys is reported, based on production of slugs for irradiation at Chalk River[30] and for the Plutonium Recycle Test Reactor (PRTR) program at Hanford.[31] The constitution and metallurgy of aluminum-plutonium alloys are quite similar to those of aluminum-uranium alloys. Thus this work benefits greatly from the uranium experience.

Two methods of making the alloys by coreduction have been developed. The first method is to reduce plutonium fluoride with aluminum.[30] Best results were obtained at 900°C, using charges containing 30 to 60 g of plutonium. Yields of 98 per cent were obtained. These reductions were carried out in vacuum, and the reaction rate at 900°C, where aluminum monofluoride is volatilized, is five times that at 1125°C, where aluminum trifluoride is volatilized.

The second method of coreduction consists of reduction of plutonium dioxide with aluminum. First tests[30] indicated that reaction is retarded by formation of a barrier of Al_2O_3. Cryolite was then charged to dissolve the Al_2O_3. The process has gone through various steps of development using the cryolite addition. The present process consists of adding powdered PuO_2-cryolite mixtures to a cold graphite crucible. After addition of the aluminum and a covering layer of cryolite, the assembly is heated 15 min at 1200°C and cooled. The plutonium yield on routine production of aluminum–3.7 wt.% plutonium alloy batches containing 30 g of plutonium is consistently better than 99.5 per cent.[30] The composition is, of course, controlled by addition of the appropriate excess of aluminum. The process has also been adapted for the production of slugs for the PRTR.[32]

Plutonium-aluminum alloys have also been made successfully by addition of plutonium to molten aluminum in open pot type furnaces.[32] The plutonium is protected from oxidation by submersion in the aluminum, and any oxide present is reduced by the aluminum.

In general, these alloys, up to the eutectic composition 1.7 at.% plutonium, are easily cast and quite workable. During casting of the alloys, there is an increasing tendency with increasing plutonium composition to develop gravity segregation by settling of the dense $PuAl_4$ phase, similar to aluminum-uranium alloys. This tendency has been minimized by casting into water-cooled copper molds and by careful adjustment of pouring rates and temperatures.[30]

At Hanford[31] 12-in. sections of ½-in.-diameter rods of 1.8, 10, and 15 wt.% plutonium have been vacuum cast with a minimum of segregation and piping by pouring into graphite molds. Similar casting studies at Chalk River[30] with a 3.7 wt.% plutonium alloy gave satisfactory ingots 1.43 in. in diameter (mold length 14 in.). These ingots were made by pouring into tilted molds to avoid splashing and resultant porosity. The plutonium concentration variation top-to-bottom was about 5 per cent, and some tendency toward inverse segregation at the surface was observed. Loss of plutonium as oxide was about 2 per cent.

Limited data are reported for irradiation of aluminum-plutonium alloys. Irradiations have been performed to burn-ups of 55 to 60 per cent of the plutonium in a 20 wt.% plutonium alloy (1.5 at.% total) jacketed in aluminum.[30] The irradiated assemblies contained slugs varying in composition from 0.5 to 20 wt.% plutonium. In subsequent irradiations difficulty was encountered after a few months of service, but too few data are available to explain the cause. At Hanford[31] preliminary irradiations of ½-in.-diameter slugs, 2 in. long, of a 1.64 wt.% plutonium alloy and of a 12 wt.% silicon–1.61 wt.% plutonium ternary alloy are reported. The irradiations are reported to be successful at about 20 at.% burn-up of the plutonium, and no instability nor dimensional changes were observed, although hardnesses increased from 50 to 94 R_H and 86 to 102 R_H for the binary and ternary alloys, respectively. Burn-ups of 55 to 60 at.% of the plutonium are in progress. The silicon addition is included because of enhanced high-temperature-water corrosion behavior; details were not included.[31]

Plutonium-Thorium

Studies at Harwell[33] have resulted in a completed constitutional diagram for this system based on various examination techniques.

Plutonium dissolves extensively in alpha thorium, the maximum solubility being 45 at.% plutonium at 615°C. At about 32 at.% thorium a compound occurs which is probably orthorhombic with a = 9.820 A, b = 8.164 A, and c = 6.681 A. This compound forms peritectically at 615°C, from the alpha thorium + liquid field, which extends over a large part of the diagram. The formation of the compound is sluggish on cooling and is normally preceded (at 605°C) by the eutectic, at about 7 at.% thorium, between epsilon plutonium, containing about 5 at.% thorium, and the compound. The remainder of the compound is then formed by a peritectoid reaction at about 580°C between epsilon plutonium and alpha thorium. Delta plutonium forms peritectoidally at 500°C by a reaction between epsilon plutonium and the compound. This reaction cannot be suppressed by quenching, and filings quenched from the epsilon field always show the X-ray diffraction pattern of delta plutonium. Maximum solubility of thorium in delta plutonium is about 5 at.% at 500°C.

A somewhat lower maximum solubility of plutonium in thorium reported previously by Argonne[34] was mentioned in the last issue of this Review.

Other Binary Alloys

Preliminary data are reported by Los Alamos[35] on the structure of $PuNi_3$, but details are incomplete. Also, a brief report[35] on titanium alloys indicates that the plutonium delta-prime phase can contain as much as 5 at.% titanium in solid solution at 450°C.

In the zinc system alloys containing 5 to 98.4 wt.% zinc have been examined.[35] Three compounds are reported with $PuZn_3$ being the richest in plutonium. The delta plutonium phase is retained at room temperature in the plutonium-rich alloys. The solubility of zinc in plutonium appears to be greater than 5 at.%.

At Argonne[36] preliminary data are reported on an arc-melted ingot of zirconium–5.7 ± 0.4 wt.% plutonium. The alloy has good fabricability. It was hot-pressed at 730°C to a 50 per cent reduction. It was then cold-rolled 97.5 per cent to 0.03-in. foil. The hardness was 43 R_A (68 R_B) as cast and 53 R_A (86 R_B) after 50 per cent reduction.

Uranium-Plutonium-Fissium

Additional data are reported at Argonne on the uranium-plutonium-fissium alloys.[9] Al-

though the alloys are intended for use in the as-cast condition, studies of fabricability were performed as general background on the characteristics of the alloys. The following alloys were included:

Uranium–20 wt.% plutonium–10.8 wt.% fissium
Uranium–20 wt.% plutonium–5.4 wt.% fissium
Uranium–20 wt.% plutonium–5.4 wt.% fissium–3.6 wt.% molybdenum
Uranium–20 wt.% plutonium–5.0 wt.% molybdenum

Fissium compositions indicated in the above alloys are as follows:

	10.8 wt.%	5.4 wt.%
Molybdenum	2.8	1.40
Zirconium	0.50	0.25
Ruthenium	4.30	2.15
Rhodium	0.70	0.35
Palladium	2.50	1.25

All the alloys were extruded successfully by the inverse extrusion process using bare billets and a 7-to-1 reduction at 390 to 500°C. Mean thermal-expansion coefficients for the uranium–20 wt.% plutonium–5 wt.% molybdenum alloy are as follows:

Temperature range, °C	Mean thermal-expansion coefficient, 10^{-6} in./(in.)(°C)
25–391	15.91
25–532	17.61

A change in slope of the expansion coefficients indicates the alloy undergoes transformation at 560 to 572°C. (F. A. Rough)

Thorium Alloys

In a report by Raynes et al.,[37] additional details are given on the properties of high-purity thorium prepared by electrolysis of thorium chloride. Arc-melted thorium prepared by this method has a hardness of 70 to 80 DPH; and, as cold-rolled and annealed for 1 hr at 600°C, it has a yield strength of 41,700 psi, an ultimate strength of 52,200 psi, and 11 per cent elongation in 1 in. These data suggest that electrolytic thorium can be produced having properties equivalent to those of bomb-reduced thorium. Photomicrographs and accompanying analyses for "HCl-insoluble" material show hardness changes from 11 to 70 Rockwell B with increasing oxygen content (insoluble material increasing from 1.2 to 11 per cent).

In attempts to clad thorium with Zircaloy-2 and to improve the corrosion resistance of the composite element, Nuclear Metals reports[38] that diffusion between thorium and zirconium is exceedingly rapid at 1000°C and that the diffusion layers obtained were harder than either the Zircaloy or the thorium. Stud tests of the Zircaloy-thorium bond showed that the thorium core was the weakest member of the clad composite. Attempts to strengthen the thorium with carbon did not change the results of the stud tests; however, corrosion tests showed that increasing the carbon content of as-extruded thorium from 0.07 to 0.64 per cent decreases the corrosion rate in 500°F water from 80 to 20 g/(cm^2)(month). Other tests showed that increasing the zirconium content of as-cast thorium from 25 to 75 per cent decreases the corrosion rate in 500°F water from 5.5 to 0.8 g/(cm^2)(month).

New Brunswick Laboratories, Inc.,[39] has identified one of the inclusions in thorium as an iron-nickel-cobalt phase having the general formula Th_7M_3, where M represents iron, cobalt, and nickel. This constituent is described and differentiated from ThO_2 in terms of microstructures and appearance. The iron phase is described as silvery white and predominates in the grain boundaries but occasionally is found dispersed to some extent. Thorium oxide, on the other hand, is described as being gray to black, appearing in dendritic form in castings and as stringers, clusters, and blobs in wrought metal.

In studies of the decontamination of irradiated thorium by melting, Atomics International Div.[40,41] finds the vapor pressures of thorium and protactinium at 2200°K to be 4.2×10^{-6} atm and 5.1×10^{-5} atm, respectively.

Ames has reported results of constitutional-diagram studies in several thorium systems. A nearly isothermal ternary eutectic trough was found between the aluminum-uranium eutectic at 640°C and the aluminum-thorium eutectic at 632°C. It is suspected that a low point

occurs in this ternary eutectic trough[27] at 630°C and 76 wt.% aluminum, 18 wt.% thorium, and 6 wt.% uranium. Hydrogen is reported[15] to be soluble in thorium to the extent of 21 at.% at 775°C. The thorium-molybdenum system is apparently analogous to the thorium-chromium system; there are no thorium-molybdenum compounds, and a eutectic[15] exists near 1400°C. The thorium-hafnium system has been determined and seems to be intermediate in nature to the thorium-titanium system and the thorium-zirconium system. A eutectic reaction occurs at 26 wt.% hafnium and 1450°C, producing beta thorium containing 13 wt.% hafnium and alpha hafnium containing about 2 wt.% thorium. An inverse peritectic is postulated at 1600°C and 96 per cent hafnium, forming alpha hafnium containing 2 wt.% thorium and liquid containing 60 per cent thorium. A eutectoid was located at 1295°C and 9 per cent hafnium. On cooling, this reaction produces alpha thorium containing 5 wt.% hafnium and alpha hafnium containing 2 wt.% thorium.[42] In connection with studies aimed at reprocessing thorium fuels by pyrometallurgical means, additional data have been obtained on the ternary uranium-thorium-magnesium system. The solubility of uranium in magnesium–16 wt.% thorium solution at 650°C is 0.004 wt.% at 650°C and is 0.14 wt.% at 1132°C. The solubility[43] of uranium in magnesium–35 wt.% thorium solution is 0.007 wt.% at 650°C and is 0.14 wt.% at 1132°C.

Additional data from Harwell[33] and Argonne[34] have clarified considerably the details of the thorium-plutonium constitution diagram. On the basis of information from both laboratories, it appears certain that there is a eutectic at 605°C and 93 at.% plutonium. On cooling, this reaction produces epsilon plutonium containing about 5 at.% thorium and the single intermetallic phase Pu_2Th. On heating, the phase Pu_2Th decomposes at 615°C into liquid containing almost 93 at.% plutonium and alpha thorium containing more than 35 and less than 45 at.% plutonium. From this information it appears that the transformation of beta thorium to alpha thorium must occur by an inverse peritectic reaction in this system, but a temperature for this reaction has not been disclosed.

Irradiation data on thorium and thorium-uranium alloys continue to indicate a marked superiority of thorium-base fuels over uranium-base fuels. Savannah River reports[44] that 60 thorium slugs irradiated at Hanford to a conversion of 800 ppm of Th^{232} showed no damage. Thirty-two slugs irradiated to a conversion of 2800 ppm of Th^{232} showed no evidence of gross dimensional instability. The fission burn-up of U^{233} produced in the thorium can be estimated as somewhat less than 40 per cent of the Th^{232} converted.

Hanford reports[45] that a thorium–2.1 wt.% U^{235} slug irradiated in the MTR was sufficiently intact for mechanical tests. A slug 1.5 in. long and 0.39 in. in diameter given a cantilever bend test on 1-in. centers broke in a brittle fashion at a 5060-lb load and 0.040-in. deflection. During irradiation the alloy increased in hardness from 40 to 59 Rockwell A. It is not clear whether this slug was from a group of thorium–2 wt.% U^{235} alloys which received ½ at.% burn-up or whether it received 1 at.% burn-up. Other irradiations of enriched-thorium alloys are in progress or planned.

(W. Chubb)

Dispersion Fuel Materials

Work on dispersion fuel elements now involves many material combinations; however, the stainless-steel–UO_2 system continues to receive the greatest attention.

A Sylvania-Corning[46] report describes in detail the fabrication of several 17-in.-long tubular elements containing cores of 5.6 wt.% UO_2 dispersed in type 302B stainless steel clad with type 347 stainless steel. The cores were prepared by compacting, sintering, and recoining bushinglike segments approximately 0.50 in. long having an outside diameter of 0.46 in. and an inside diameter of 0.25 in. These segments, having a theoretical density of 95.5 per cent, were electrolytically nickel plated and stacked between two type 347 stainless-steel tubes, along with appropriate end plugs. The welded assemblies were given a light reduction through a drawing die and were then heated to 1100°C for 30 min, allowing the nickel alloy plate to braze the core to the cladding. Although the tubes were prepared for sensing devices, the techniques described are also applicable to fuel-element fabrication.

A program has been initiated at Knolls to develop a fuel element using stainless steel as

the cladding material and a stainless-steel–UO_2 core. A modification of the cold binder extrusion process developed at Knolls will receive the primary fabrication effort. In this process the core materials are premixed into a plastic mass, cold-extruded, and sintered to about 70 per cent of theoretical density. The cylindrical cores are canned in stainless steel and are hot-worked through a series of grooved rolls followed by Turk's heading to final size. Further work will employ rectangular cores and a power-driven Turk's head for all operations.

Table I-2 TYPES OF IRRADIATION SAMPLES* IN PROGRAM ON ADVANCED DEVELOPMENT OF ZIRCONIUM-BASE FUELS (KNOLLS DATA)

Particle size, μ	Samples
	Slugs 1 and 2
40	Uranium particles in Zircaloy-3
200	UO_2 particles in Zircaloy-3
200	Uranium particles
200	UO_2 particles
200	Uranium particles in Zircaloy-3
40	UO_2 particles in Zircaloy-3
	Uranium-zirconium alloys (1 μ UZr_2 particles in zirconium-uranium solid solution)
	Slugs 3 and 4
40	Uranium particles in Zircaloy-3
200	UO_2 particles in Zircaloy-3
200	Uranium particles
200	UO_2 particles
200	Uranium particles in Zircaloy-3
40	UO_2 particles in Zircaloy-3
200	UC particles
200	UC particles in Zircaloy-3
40	UC particles in Zircaloy-3
	Uranium-zirconium alloy (1 μ UZr_2 particles in zirconium-uranium solid solution)
200	UZr_2 particles
	Slugs 5 and 6
200	UC particles
200	UC particles in Zircaloy-3
40	UC particles in Zircaloy-3
200	UC particles in zirconium-uranium solid solution
200	UO_2 particles in zirconium-uranium solid solution
200	Uranium particles in zirconium-uranium solid solution

*Total number of samples was 72; uranium concentration was 5 at.% in all samples except particles alone.

An advanced development program at Knolls is concerned with the effect of microstructure and composition on the irradiation stability of zirconium-base fuels. The systems investigated are dispersions of uranium, UO_2, UC, and UZr_2 phases in a zirconium alloy matrix phase. Plans for the present irradiation program call for the irradiation of 72 specimens at the MTR at burn-ups of 0.7 to 2.2 at.%. The specimens are grouped statistically in six irradiation slugs (multiple capsules), as indicated in Table I-2. All specimens have been fabricated, and the first two slugs were inserted in the MTR around Sept. 1, 1957.

Small uranium-magnesium dispersion elements canned in Zircaloy-2 containing 50 vol.% uranium were irradiated to 20,000 Mwd/ton (2.32 at.% burn-up in the uranium) without dimensional changes. The restraint of the heavy Zircaloy-2 can was thought to resist swelling. Recent postirradiation examination of uranium-magnesium fuel elements canned in aluminum have shown a 3.25 vol.% expansion during an exposure of only 800 Mwd/ton (0.08 at.% burn-up of uranium). These results are similar to those obtained with Knolls specimens (Table I-3). As yet there is no apparent explanation of the observed swelling in either set of specimens.

Work is continuing at Oak Ridge[47] on the development of aluminum-base fuel elements

Table I-3 SWELLING DATA ON POWDER-METALLURGY URANIUM-MAGNESIUM

Sample	Exposure, Mwd/ton	Preirradiation diam., in.	Postirradiation diam., in.			Calculated volume increase, %
			Min.	Max.	Av.	
25-H	1000	0.3480–0.3485	0.349	0.358	0.353	2.63
45-H	1000	0.3480	0.352	0.360	0.356	4.41
26-H	3000	0.3485–0.3490	0.359	0.371	0.366	9.74
30-H	3000	0.3480–0.3485	0.364	0.369	0.366	10.2
44-H	3000	0.3470	0.360	0.365	0.362	8.56

containing dispersions of both UO_2 and U_3O_8. A recent report describes some interesting developments in this field. Manufacturing specifications for aluminum-base fuel elements call for an extended anneal at 600°C after hot and cold working. Figure 3 illustrates the major problem encountered during the initial work with dispersed UO_2 fuel material for the Geneva reactor. The oxide reacted with the aluminum to form UAl_3, UAl_4, and Al_2O_3. This reaction was accompanied by a significant volume increase, causing a high rejection of elements. Recent work has shown that, if U_3O_8 is substituted for the UO_2, a reaction takes place forming significant quantities of UO_2 (Fig. 4). However, this dioxide is apparently stable in aluminum, and Fig. 3 shows that the total volume change is negligible. (D. L. Keller)

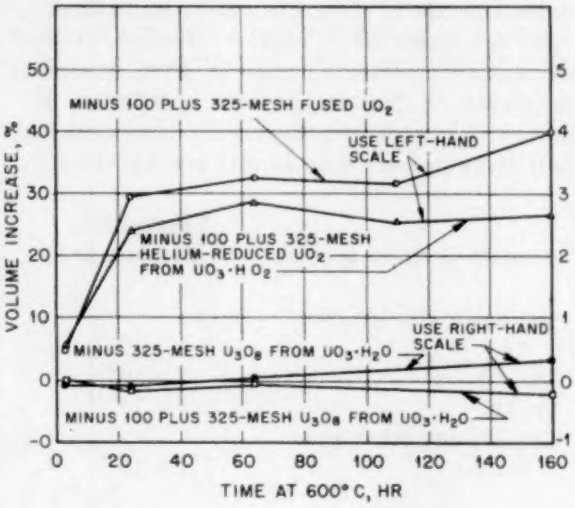
MINUS 100 PLUS 325-MESH FUSED UO_2
USE LEFT-HAND SCALE
MINUS 100 PLUS 325-MESH HELIUM-REDUCED UO_2 FROM $UO_3 \cdot H_2O$
USE RIGHT-HAND SCALE
MINUS 325-MESH U_3O_8 FROM $UO_3 \cdot H_2O$
MINUS 100 PLUS 325-MESH U_3O_8 FROM $UO_3 \cdot H_2O$
VOLUME INCREASE, %
TIME AT 600° C, HR

Fig. 3—Growth characteristics of 52.3 wt.% UO_2 and 55.7 wt.% U_3O_8 aluminum fuel plates.[47]

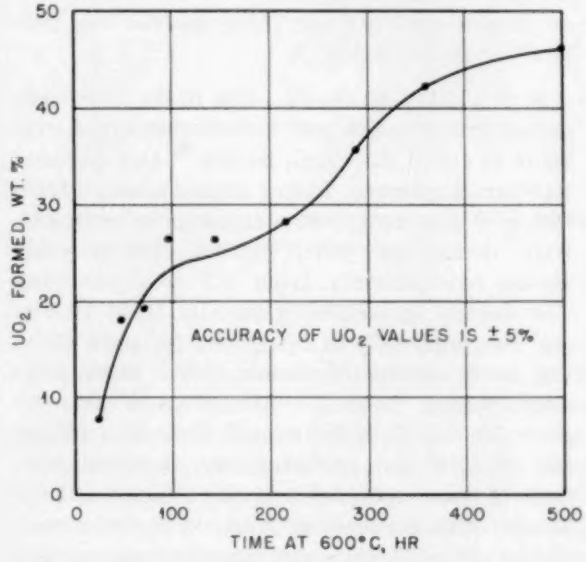

Fig. 4—UO_2 formation during heat-treatment of 56.4 wt.% U_3O_8 aluminum plate.[47]

Refractory Fuel and Fertile Materials

Fabrication of UO2-containing Bodies

In work at Chalk River[48] the density of pellets made from UO_2 powders prepared by hydrogen reduction of ammonium diuranate was found to depend on the conditions under which the ammonium diuranate was precipitated. The study resulted in specifications for preparing UO_2 powder that sintered to a density greater than 10.0 g/cm^3 when compacted at 40,000 psi and sintered at 1600 to 1700°C for 1 hr.

Hydration of MCW type UO_3 by wet milling increased the sinterability of UO_2 powder made by hydrogen reduction of the trioxide, according to a paper by Vaughan et al.[49] The density of compacts formed from this powder at 20,000 psi and sintered in hydrogen for 1 hr at 1650°C was reported to be 10.4 g/cm^3. It was also reported that the sinterability of UO_2 powders was directly related to their tendency to increase in oxygen to uranium ratio at room temperature.

Murray et al.[50] compacted nonstoichiometric oxides ranging from UO_2 to U_3O_8 at 14,000 to 20,000 psi and sintered them in argon, nitrogen, hydrogen, carbon monoxide, or vacuum. No details of methods of preparing the powders were given. The most sinterable of the oxides evaluated, U_3O_8, had a density of 10.8 g/cm^3 after sintering for 1 hr in argon at 1200°C. The U_3O_8 was reduced to $UO_{2.26}$ during sintering. There also was evidence of some uranium loss during sintering. Considerably higher temperatures were required to obtain equivalent densities when sintering was done in hydrogen. (H. D. Sheets)

Properties and Behavior of Uranium Oxide Fuels

1. *Uranium Dioxide.* Excellent summaries of Bettis work on UO_2 properties[51] and the effects of radiation[52] on bulk UO_2 have been published recently. Most of the UO_2 data pertinent to reactor applications are reviewed prior to late 1957 in these two summaries. Literature references on UO_2 technology and irradiation effects have been compiled by Ferrier.[53]

The kinetics of the oxidation of UO_2 to U_3O_8 in the temperature range 160 to 350°C was reported by Aronson et al.[54] Oxygen diffusion through the UO_2 lattice and its role in the oxidation mechanism are discussed.

A study of structural and compositional variations in uranium oxides is being continued at Battelle.[20] Electrical-property data have been obtained on a series of UO_2 specimens containing small additions of CaO, ZrO_2, and MoO_3. CaO produces a marked reduction in room-temperature resistivity, which is consistent with the substitution of a bivalent calcium ion for a tetravalent uranium in the fluorite lattice. Tetravalent zirconium ions, as expected, show little effect on the resistivity. Hexavalent molybdenum ions are responsible for increased resistivity as they are apparently reduced in valency by the UO_2.

The thermal conductivity[28] and strength of UO_2 bodies are being studied by Bettis and Hanford, respectively. In the Bettis program the radial temperature drop across a thermocoupled UO_2 pellet will be monitored during irradiation. Hanford has initiated a study of thermal shock and impact failures in sintered UO_2 slugs. The mechanism of fracture will be studied by surface examination of the fracture areas. No results have been reported for either of these two studies.

In a recent British paper[50] possible effects of the oxygen-uranium ratio on the high-temperature irradiation performance of sintered UO_2 bodies are discussed. Nonstoichiometric UO_2 has higher volatility, lower creep strength, and lower sintering temperature than stoichiometric UO_2. At high temperature it is suggested that these factors may contribute to greater mass transfer and to dimensional and microstructure changes in nonstoichiometric UO_2 fuel bodies.

Irradiation of clad UO_2 pellets in pressurized-water loops and the parameters important to fuel-rod integrity have been summarized.[55] The significance of fission-gas release from UO_2 pellets has been studied at Bettis.[56] Power cycling of defected blanket rods increases fission-gas release tenfold. During one core life the estimated maximum number of defected rods is 1000. Only 30 of these defected rods are expected to rupture. Fission-product escape from defected rods is often described in terms of the escape-rate coefficient. Reported values for fission-product isotopes having half lives greater than 30 min are listed below.

Fission-product species	Escape-rate coefficient, sec^{-1}
Cs, I, Br, Rb, Kr, Xe, Te	1×10^{-8}
Mo	2×10^{-9}
Sr, Ba	1×10^{-11}
Ce, Zr, and other rare earths	2×10^{-12}

Booth[57] has discussed the calculation of fission-gas release from UO_2 slugs. Calculated values are sensitive to the theoretical model selected and to the value of the centerline temperature of the slug. The effect of UO_2 density on fission-gas release from natural UO_2 pellets[16] is shown in Fig. 5.

2. *UO_2-ThO_2 Mixtures.* Oak Ridge is investigating the strength and high-temperature stability in air of UO_2-ThO_2 bodies.[58] Dry-pressed flat-bar specimens, having urania contents from 100 to 0 per cent, were sintered in hydrogen. With increasing ThO_2 content, the porosity varied nonuniformly from 0.7 to 2 per cent. The density decreased gradually from 10.0 g/cm^3 for pure UO_2 to 8.9 g/cm^3 for pure ThO_2. The sonic moduli of elasticity for these mixtures ranged from 16×10^6 to 28×10^6 psi. For pure UO_2 and ThO_2 the moduli were 25×10^6 psi and 30×10^6 psi, respectively. Selected portions of these specimens were refired at 1800°C in air with no soaking time. Specimens containing 10 wt.% ThO_2 disintegrated during this test. For a specimen containing 20 wt.% or more of ThO_2, weight losses were less than 1 per cent.

3. *UO_2-Y_2O_3 Mixtures.* The UO_2-Y_2O_3 system has been investigated by X-ray powder techniques by Ferguson and Fogg at Harwell.[59] A range of solid solutions with pseudo-fluorite

structures exists between 0 and 78 mole % of $YO_{1.5}$. There is an immiscibility gap between 78 and 96 mole % of $YO_{1.5}$. Density measurements show all these solid solutions have an anion-vacancy structure.

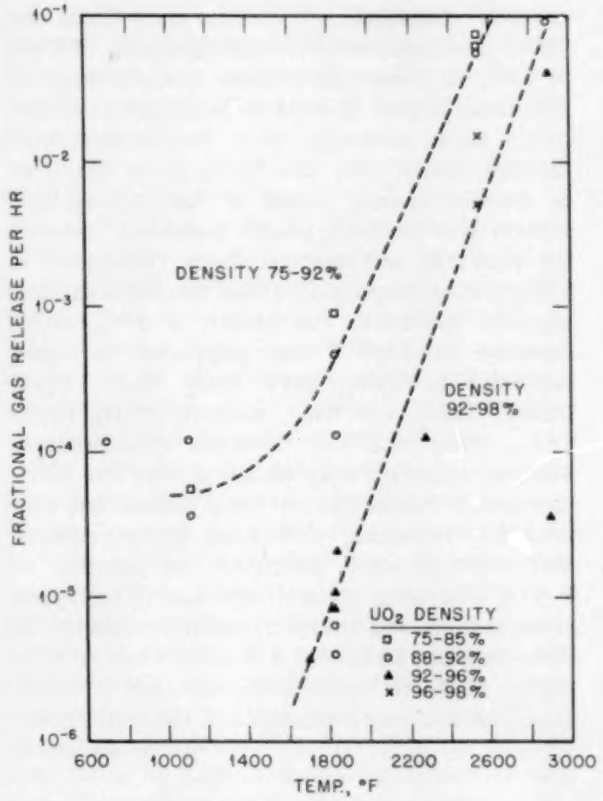

Fig. 5—Fission-gas release from natural UO_2. Bettis data, compiled by the Naval Reactors Branch.[16]

4. *UO_2-Al_2O_3 Mixtures.* Ceramic plate type UO_2-Al_2O_3 seed fuel containing 80 to 85 wt.% Al_2O_3 is being studied at Bettis.[60] Several specimens compartmented in Zircaloy-2 have been irradiated to estimated uranium burn-ups of 16 at.%. The theoretical densities of these specimens were 95 to 98 per cent. Preliminary fission-gas-release experiments indicate that these UO_2 mixtures release three to five times more fission gas than UO_2 of comparable density.

5. *UO_2-PuO_2 Mixtures.* As part of an irradiation program on candidate fuels for a fast-breeder reactor, Knolls has investigated 80 wt.% UO_2-PuO_2 mixtures.[61] Fully clad pellets having a theoretical density of 65 per cent were irradiated to plutonium depletions of 5 and 35 at.% at temperatures of 600 and 300°C, respectively. The gap between the 30-mil cladding and the pellets was filled with helium. Centerline voids in the pellets, but no cladding distortion, were observed under these conditions. Postirradiation examination also showed pellet shrinkage and a resulting increase in the gap between the pellets and the cladding. When a lead thermal bond was used in place of the helium, no void formation was observed in the irradiated pellets. However, the pellets did assume a "dried mud flat" appearance under these conditions.

6. *U_3O_8-SiO_2 Mixtures.* Irradiation studies on uranium oxide–glass fuels have been summarized in a recent report.[62] Commercial uranium glass containing 10 wt.% of enriched U_3O_8 and Vycor impregnated with up to 10 wt.% of natural or enriched U_3O_8 were irradiated in the program. Uranium burn-up was 15 at.%, and surface temperature was 200°C in the commercial-glass specimens. The temperature gradient across these latter ¼-in.-O.D. specimens was 1500°C. Although the softening point (1450°C) of the Vycor was probably reached in these ¼-in.-O.D. specimens, no appreciable fission gas was released. The temperature of the impregnated specimens ranged from 650 to 830°C during irradiation. U^{235} burn-up was 5 to 15 at.%. Fission-gas release in these specimens was also low. Postirradiation examination showed severe cracking in many of the specimens made from both types of uranium oxide–glass fuel. (W. S. Diethorn)

Fabrication of Uranium Carbide

Continued investigations reported by Battelle[63] resulted in refinement of fabrication processes for UC. Sintered compacts with densities greater than 98 per cent of theoretical were made by compacting finely ground UC powder hydrostatically at 100,000 psi and sintering for about 3 hr in vacuum at about 1850°C. The observed reduction in porosity of the sintered compacts was attributed to the prolonged sintering time and the use of finely ground UC powder as starting material.

(J. F. Quirk)

Properties of Refractory Fuels Other than Uranium Oxides

Battelle[20,64,65] has investigated the physical properties of several uranium compounds and determined their stability in atmospheres of nitrogen, oxygen, and water vapor. The thermal-expansion coefficients of the silicides and of UAl_2 were approximately equal and were of the same order of magnitude as that of uranium metal. Specific heats range from about 0.04 cal/(g)(°C) for U_3Si to about 0.08 cal/(g)(°C) for USi_3. The microhardness of USi_3 was appreciably lower than that of the other silicides. Rates of reaction of oxygen with UBe_{13}, UB_2, and USi_2 increase in that order and initially follow a linear rate law up to 400°C. Above 400°C, UB_2 and USi react anisothermally which results in complete combustion in a short time. In contrast, UBe_{13} reacts isothermally up to 600°C. The reaction stopped almost entirely before complete oxidation occurred. The reactions of the compounds USi_3, U_3Si_2, USi_2, and UC_2 with oxygen follow a parabolic rate law up to 400°C, the rates increasing in the order listed, whereas the oxidation of UAl_2 follows a cubic law. Pure uranium oxidizes linearly at these temperatures. The reaction of nitrogen with these compounds follows a parabolic law at temperatures up to 600 or 800°C. UB_2 was the only material that reacted more slowly with nitrogen than did uranium under similar conditions. However, in all cases, the reactions of the compounds with nitrogen were slower than those with oxygen at the same temperature. Reactions of water vapor at a pressure of 29 mm Hg with UBe_{13}, UB_2, and UC_2 follow a linear rate law with the exception of those with UC_2. These reactions are slower than the reactions of oxygen with the compounds.

The thermal stabilities of compounds in the systems uranium-zirconium-silicon and uranium-carbon-nitrogen are being investigated at Battelle.[65] Tentative lattice-parameter data are given for the solid-solution phase $(U,Zr)_3Si_2$. X-ray data on solution-treated samples of UC-UN mixtures indicate complete miscibility of these two isostructural compounds.

Investigations on ceramic materials containing thorium are in progress. The ThO_2-SiO_2 system is being studied at Oak Ridge.[58] Although two polymorphic modifications of $ThSiO_4$ have been reported to occur in nature, only the monoclinic phase has been synthesized. This compound dissociates into ThO_2 and glass on heating to 2000°C. Duwez[66] showed a large (83 mole %) solid solubility of cubic ZrO_2 in ThO_2 at very high temperature. However, during prolonged heating at 2000 or 1350°C, the solid solution dissociates to nearly pure ZrO_2 and ThO_2. The equilibrium solid solubility of ThO_2 in ZrO_2 is somewhat greater in the tetragonal modification than in the low-temperature monoclinic form. Although these bodies have high melting points, they are likely to be sensitive to thermal shock, owing to the polymorphic inversion of the ZrO_2 phase. Arenberg[67] studied the sintering and thermal-shock resistance of ThO_2 bodies containing small amounts of isomorphic additives. The density of ThO_2 bodies sintered at 1500°C was improved by small additions of CaF_2, SrF_2, SnO_2, Bi_2O_3, V_2O_5, $CaBr_2$, $CaCl_2$, and NH_4I, whereas Pb_3O_4, PbF_2, ThF_2, ThF_4, and UO_2 retarded densification. Vacuum sintering aids densification. The thermal-shock resistance of ThO_2 bodies was improved by replacing −325-mesh starting powder with −40 +60-mesh particles. An addition of 5 wt.% stabilized ZrO_2 (−325 mesh) improved densification and thermal-shock resistance of ThO_2 bodies. However, a 5 wt.% addition of Al_2O_3, MgO, or pure ZrO_2 resulted in lower densities and less resistance to thermal shock.

(D. A. Vaughan)

Basic Studies of Radiation Effects on Fuel Materials

In the last issue of this Review the work at Bettis[68] on the diffusion of fission gases in UO_2 was discussed. The activation energy for diffusion of fission gases was reported to be similar to that for diffusion of oxygen in UO_2 (about 20 kcal/mole). This indicated the possibility that fission-gas diffusion was related to the oxygen-diffusion mechanism. In a more recent report[52] reviewing the work on UO_2, evaluation of the results on fission-gas release has led to a different interpretation. The activation energy for fission-gas diffusion is shown to be about 1 kcal/mole below about 1000°C and about 100 kcal/mole above this temperature. It was tentatively concluded that fission gases have the mobility of cations and diffuse by a

similar mechanism at high temperatures but diffuse by a different mechanism below 1000°C. Comparison is made with results of studies of diffusion of radon in alpha Al_2O_3, in which similar behavior was observed. In this case the interpretation is given that at high temperatures the activation energy consists of the energy required for mobility of the diffusing gas and the energy required to form defects, whereas at low temperature the activation energy consists only of the energy required for mobility.[69]

The effect of irradiation on crystal properties of UO_2 is also discussed.[52] Specimens of UO_2 of different particle and crystallite sizes and specimens of U_4O_9 and U_3O_8 irradiated to levels of 100 Mwd/ton or less approached the same crystallite size after irradiation regardless of initial size. Disordering of the lattice by fission or displacement spikes and subsequent reordering on the matrix lattice is offered as a possible explanation of this behavior.

The formation of gas bubbles in Perspex (polymethyl methacrylate) by thermal depolymerization and radiation has been studied to provide some insight into the mechanism of internal bubble formation in solids.[70] This material was selected because it evolves gas as a result of thermal decomposition and radiation damage, and its transparency permits visual observation of bubble formation and growth. It was concluded from this investigation that, at low rates of gas formation, gas bubbles are formed at defect sites after the gas concentration exceeds a certain critical value. However, if the rate of gas formation is sufficiently high that the diffusion distance at the particular temperature and time required to exceed the critical concentration of gas is small compared to the distance between defect sites, a larger number of smaller bubbles are formed. If these gas bubbles are sufficiently small, the surface tension as well as the bulk strength of the solid would constrain the bubbles and prevent swelling of the solid. Irradiation at high flux and low temperature would favor this condition.

Investigation of bubble formation in ٦ fuel material was conducted by heat treating small pieces of natural-uranium fuel bars from the NRX reactor at Chalk River which were irradiated to a 0.3 to 0.4 at.% burn-up at temperatures[6] below 200°C. On heating in vacuum at 575°C, a 2 vol.% increase was obtained, and at 810°C the volume increased by 5 per cent. Thermal cycling at 810°C produced volume increases as large as 15 per cent.

Examination of the swollen metal with optical and electron microscopes revealed bubble sizes in the range 5×10^{-6} to 10^{-2} cm in diameter. The majority of the gas volume was in the smaller bubbles, and the total void volume was sufficient to account for the observed amount of swelling. It was concluded that swelling at high temperature is less in those specimens in which the gas bubbles are smallest, due to the restraining effect of the surface tension of the fuel material. However, the relative importance of surface tension and bulk strength of the fuel material may well be different for large fuel specimens than it is for the small specimens used in the Harwell investigation.

(P. Schall, Jr.)

References

1. W. R. McDonell, Kinetics of the Beta Transformation of Uranium, DP-230, September 1957. (Unclassified AEC report.)
2. A. L. Bement and W. P. Wallace, A Martensitic Reaction for Uranium, HW-51084 (Rev.), June 25, 1957. (Unclassified AEC report.)
3. G. W. Powell, J. L. Klein, and D. Krashes, Grain Refinement of Cast Uranium by Heat-Treatment, NMI-1180, July 5, 1957. (Confidential AEC report.)
4. John W. Simmons, editor, Summary Technical Report for the Period July 1, 1957, to September 30, 1957, NLCO-690, October 1957. (Confidential AEC report.)
5. J. H. Kittel and S. H. Paine, Effects of High Burn-up on Natural Uranium, ANL-5539, May 1, 1957. (Unclassified AEC report.)
6. A. T. Churchman, R. S. Barnes, and A. H. Cottrell, Effects of Heat and Pressure on the Swelling of Irradiated Uranium — Part I, AERE-M/R-2044, 1956. (Unclassified British report.)
7. B. E. Hopkinson, Kinetics of the Uranium–Steam Reaction, AERE-M/R-1281A, January 1957. (Unclassified British report.)
8. R. F. S. Robertson, Defect Test on Uranium–2 Wt. % Zirconium Alloy in X-2 Loop Test No. 2, CRDC-647, May 1957. (Unclassified Canadian report.)
9. Metallurgy Division Quarterly Report for October, November, and December, 1956, ANL-5709, Dec. 31, 1956. (Confidential AEC report.)
10. J. R. Murray and S. J. Lloyd, Some Observations on Uranium-rich Uranium-Ruthenium Alloys, AERE-M/M-107 (Del.), January 1956. (Unclassified British report.)

11. *Nuclear Metallurgy*, Symposium on Uranium and UO_2, Vol. 4, American Institute of Metallurgical Engineers, November 1957.
12. R. W. Nichols, Uranium and Its Alloys, *Nuclear Engineering*, 2: 355-364 (September 1957).
13. S. H. Bush, Irradiation Effects in Uranium, HW-51444, July 19, 1957. (Unclassified AEC report.)
14. A. E. Dwight and M. H. Mueller, The Constitution of Uranium-rich Uranium-Niobium and Uranium-Niobium-Zirconium Systems, ANL-5581, October 1957. (Unclassified AEC report.)
15. Semiannual Summary Research Report in Metallurgy (July–December 1956), ISC-835, Aug. 23, 1957. (Unclassified AEC report.)
16. W. H. Wilson and T. O. Ziebold, Performance of Fuel Elements at Elevated Temperatures, WASH-741, Sept. 4, 1957. (Confidential AEC report.)
17. M. L. Bleiberg, J. D. Eichenberg, R. H. Fillnow, and L. J. Jones, Development and Properties of Uranium-base Alloys Corrosion Resistant in High-temperature Water, Part IV, Radiation Stability of Uranium-base Alloys, WAPD-127, May 1957. (Unclassified AEC report.)
18. E. S. Foster, Uranium–12 Wt. % Molybdenum Homogeneity and Density, WAPD-PWR(FEM)-78, Jan. 21, 1956. (Unclassified AEC report.)
19. F. R. Lorenz, Bibliography of Uranium-Molybdenum Fuel-element Program, WAPD-NCE-3308, Jan. 31, 1957. (Unclassified AEC report.)
20. R. W. Dayton and C. R. Tipton, Jr., Progress Relating to Civilian Applications During November 1957, BMI-1238, Dec. 1, 1957. (Unclassified AEC report.)
21. Monthly Technical Progress Report for February 1957, SCNC-244-P, Apr. 11, 1957. (Secret AEC report.)
22. S. Isserow, The Uranium-Silicon Epsilon Phase (Terminal Report), NMI-1160, Sept. 1, 1956. (Unclassified AEC report.)
23. Technical Progress Report to the AEC Reactor Division for the Period April 1, 1956, through June 30, 1956, NMI-1175, July 1, 1957. (Confidential AEC report.)
24. R. W. Dayton and C. R. Tipton, Jr., Progress Relating to Civilian Applications During September 1957, BMI-1226, Oct. 1, 1957. (Unclassified AEC report.)
25. Fundamental and Applied Research and Development in Metallurgy, Progress Report for April 1957, NMI-2057, May 15, 1957. (Secret AEC report.)
26. W. C. Thurber, Effects of Heat-Treatment on Microstructure and Fabricability of 48 Wt. % Uranium–52 Wt. % Aluminum Alloys, CF-57-3-160, Mar. 15, 1957. (Unclassified AEC report.)
27. G. E. Bobeck and H. A. Wilhelm, Alloys of Aluminum, Thorium, and Uranium, ISC-832, December 1956. (Unclassified AEC report.)
28. Pressurized Water Reactor Project, Technical Progress Report, WAPD-MRP-69, Aug. 23, 1957. (Unclassified AEC report.)
29. Los Alamos Scientific Laboratory and University of California Radiation Laboratory, November 1957. (Unpublished.)
30. C. J. C. Runnalls and K. L. Wauchope, The Preparation and Sheathing of Plutonium-Aluminum Fuel Alloys for the NRX Reactor, CRL-47, November 1957. (Unclassified AEC report.)
31. M. D. Freshly, Plutonium-Aluminum Fuel Element Development, Fuel Elements Conference, Paris, Nov. 18–23, 1957, TID-7546, Book 2. (Unclassified AEC report.)
32. W. L. Lyon, Hanford Atomic Products Operation, Sept. 17, 1957. (Unpublished.)
33. D. M. Poole, G. K. Williamson, and J. A. C. Marples, A Preliminary Investigation of the Plutonium-Thorium System, AERE-M/R-2156, April 1957. (Unclassified British report.)
34. Metallurgy Division Quarterly Report for July, August, and September, 1956, ANL-5643, March 1957. (Confidential AEC report.)
35. Los Alamos Scientific Laboratory and University of California Radiation Laboratory, October 1957. (Unpublished.)
36. L. T. Lloyd, Zirconium-Plutonium Alloys, Nuclear Fuels Newsletter, WASH-704, December 1957. (Confidential AEC report.)
37. B. C. Raynes, J. C. Bleiweiss, M. E. Sibert, and M. A. Steinberg, Electrolytic Preparation of Thorium Metal, *Transactions of the American Institute of Mining and Metallurgical Engineers*, 209: 1373 (October 1957).
38. S. Isserow, The Aqueous Corrosion of Zircaloy-clad Thorium, NMI-1191, Sept. 20, 1957. (Unclassified AEC report.)
39. S. J. Broderick and A. J. Busch, Metallographic Quality Studies of Thorium Metal, NBL-135, April 1957. (Unclassified AEC report.)
40. E. W. Murbach and A. G. Buyers, Decontamination of Thorium-Uranium Alloys by Nonconsumable Electrode Arc Melting, NAA-SR-1989, Sept. 1, 1957. (Unclassified AEC report.)
41. E. W. Murbach, An Estimate of the Vapor Pressures of Thorium and Protactinium, NAA-SR-1988, Nov. 1, 1957. (Unclassified AEC report.)
42. E. D. Gibson, B. A. Loomis, and O. N. Carlson, Thorium-Zirconium and Thorium-Hafnium Systems, *Transactions of the American Society for Metals*, Vol. 50, 1958. (Preprint No. 24).
43. H. E. Shoemaker and P. Chiotti, Pyrometallurgical Separation of Uranium from Thorium, ISC-841, Mar. 21, 1957. (Unclassified AEC report.)
44. R. P. Marshall, Irradiation of Thorium Slugs, DP-160, May 1956. (Secret AEC report.)
45. F. W. Albaugh, Hanford Atomic Products Operation, October 1957. (Unpublished.)
46. W. R. Weinberger and H. S. Kalish, Stainless Steel–UO_2 Dispersion Stacked Type Tubular Element for KAPL, Sept. 27, 1957.
47. R. C. Waugh and R. J. Beaver, Recent Developments in the Powder Metallurgy Application of Uranium Oxides to Aluminum Research Reactor

Fuel Elements, CF-57-9-60, Sept. 16, 1957. (Unclassified AEC report.)
48. L. C. Watson, The Production of UO_2 for Ceramic Fuels, CRL-45, Nov. 18, 1957. (Unclassified Canadian report.)
49. D. A. Vaughan, J. R. Bridge, A. G. Allison, and C. M. Schwartz, Processing Variables, Reactivity, and Sinterability of Uranium Oxides, *Industrial and Engineering Chemistry*, 49: 1699-1700 (October 1957.)
50. P. Murray, S. F. Pugh, and J. Williams, Uranium Dioxide as a Reactor Fuel, Fuel Elements Conference, Paris, Nov. 18–23, 1957, TID-7546, Book 2. (Unclassified AEC report.)
51. J. Belle and B. Lustman, Properties of UO_2, WAPD-184, September 1957. (Unclassified AEC report.)
52. J. D. Eichenberg, P. W. Frank, T. J. Kisiel, B. Lustman, and K. H. Vogel, Effects of Irradiation on Bulk UO_2, WAPD-183, October 1957. (Unclassified AEC report.)
53. M. D. Ferrier, Chalk River, 1957. (Unpublished.)
54. S. Aronson, R. B. Roof, Jr., and J. Belle, Kinetic Study of the Oxidation of UO_2, *Journal of Chemical Physics*, 27: 137 (July 1957).
55. J. D. Eichenberg, The Effects of Irradiation Cycling on Pressurized Water Reactor Blanket Fuel Elements, WAPD-167, Mar. 13, 1957. (Unclassified AEC report.)
56. W. T. Lindsay, Safeguards Aspects of PWR Reactor Coolant Chemistry, WAPD-SC-546, June 1957. (Unclassified AEC report.)
57. A. H. Booth, A Method of Calculating Fission Gas Diffusion from UO_2 Fuel and Its Application to the X-2-F Loop Test, CRDC-721, 1957. (Unclassified Canadian report.)
58. Oak Ridge National Laboratory, Dec. 13, 1957. (Unpublished.)
59. I. F. Ferguson and P. G. T. Fogg, The Oxides of Uranium. VIII. The System Uranium Dioxide-Yttria, *Journal of the Chemical Society*, 79: 3679 (August 1957).
60. Pressurized Water Reactor Project, Technical Progress Report, WAPD-MRP-70, Oct. 23, 1957. (Unclassified AEC report.)
61. W. M. Cashin, The Fast Oxide Breeder — Fuel Irradiation Experiments, KAPL-1784, Aug. 26, 1957. (Unclassified AEC report.)
62. W. M. Cashin and W. H. Howland, Knolls Atomic Power Laboratory, Sept. 9, 1957. (Unpublished.)
63. R. W. Dayton and C. R. Tipton, Jr., Progress Relating to Civilian Applications During December 1957, BMI-1247, Jan. 1, 1958. (Unclassified AEC report.)
64. M. J. Snyder and W. H. Duckworth, Properties of Some Refractory Uranium Compounds, BMI-1223, Sept. 9, 1957. (Unclassified AEC report.)
65. R. W. Dayton and C. R. Tipton, Jr., Progress Relating to Civilian Applications During October 1957, BMI-1232, Nov. 1, 1957. (Unclassified AEC report.)
66. P. Duwez and E. Loh, Phase Relationships in the System ZrO_2-ThO_2, *Journal of the American Ceramic Society*, 40: 321-324 (1957).
67. C. A. Arenberg, H. H. Rice, H. Z. Schofield, and J. H. Handwerk, Thoria Ceramics, *Bulletin of the American Ceramic Society*, 36: 302-306 (1957).
68. B. Lustman, Release of Fission Gases from UO_2, WAPD-173, March 1957. (Unclassified AEC report.)
69. W. Jost, "Diffusion," p. 314, Academic Press, Inc., New York, 1952.
70. R. S. Barnes, The Formation of Internal Gas Bubbles in Solids, *Journal of Nuclear Energy*, 5: 301 (1957).

Graphite

An investigation of materials for a power-reactor concept featuring fueled graphite elements is in progress at Battelle. The compatibility of several alloys with graphite is being assessed at BMI to provide a technical basis for selection of tubing material for coolant-gas passages through the graphite core. The following alloys appeared satisfactory from screening tests at 1850°F for 250 hr in contact with graphite: Inconel X, copper-plated Inconel X, unplated type 316 stainless steel, copper-plated type 316 stainless steel, Alnico, and chromium-plated type 316 stainless steel. These alloys will be evaluated in contact with graphite for 1000 hr at both 1850 and 1650°F.

Several graphites that are impervious to water have been prepared by the National Carbon Co. Densities range from 1.75 to 2.0 g/cm^3. Nuclear-purity tests conducted by Hanford indicate that this material has nuclear purity comparable to KC and CS grade graphite. Such a purity is generally considered satisfactory for production reactors. Impervious graphite may find application as "hardware" in future reactor designs.

(W. C. Riley)

Beryllium

Beryllium Metal and Alloys

In recent months renewed interest in beryllium as a structural material has become evident. This interest stems primarily from Air Force requirements for improved materials for airframes. Two Wright Air Development Center research projects, initiated in mid-1957, are in progress, and the first reports on this work have been received.

Alloyd Research Corporation has a contract to study the intrinsic ductility of high-purity beryllium metal. A number of techniques are to be evaluated for their ability to produce metal of the purity required. The intrinsic ductility of beryllium has never been ascertained satisfactorily since the highest purity grades developed to date contain 0.1 to 0.2 wt.% oxygen.

The methods of producing high-purity beryllium to be investigated in the Alloyd Research are (1) reduction of $BeCl_2$ with vacuum-distilled sodium; (2) zone melting, using a conventional technique (induction heating in a vacuum of 10^{-6} mm Hg) and an ultrarefined technique using electron-beam heating in an ion-pump vacuum (10^{-9} to 10^{-10} mm Hg); and (3) vacuum distillation using electron-beam heating and an ion-pump vacuum. The ultrahigh vacuum and localized heat source are deemed necessary to minimize contamination. Previous efforts to refine beryllium by vacuum distillation, using vacuums of the order of 10^{-6} mm Hg, have not been successful in producing low-oxygen material. The current research will be followed with a great deal of interest by beryllium metallurgists since it promises to answer a long-standing question whose resolution is basic to future beryllium research and technology.

The other Wright Field project has as its objective the development of improved wrought beryllium alloys and is being conducted by The Brush Beryllium Co. Specifically, it is desired to develop an alloy, retaining the high modulus of elasticity of beryllium, which can be fabricated readily into aircraft parts having improved ductility over metal of present commercial purity. The first progress report on this work includes a literature review of previous beryllium alloy development.

The Nuclear Metals study of ductility in beryllium as related to grain orientation and grain size has been summarized in a recent paper by Greenspan.[1] In the first phase of this work, the effect of fabrication procedure on texture was determined, holding grain size constant. In the second phase of the work, a study was made of the effect of grain size on the mechanical properties, utilizing approximately constant texture.

The texture developed by cross rolling after extrusion or hot pressing QMV powder is indicated, in part, by the basal-plane-pole distri-

bution shown in Fig. 6, which is reproduced from Greenspan's paper. The abscissa is the angle between the normal to the sheet surface and the basal pole (normal to the basal plane). The ordinate gives the relative X-ray intensities of

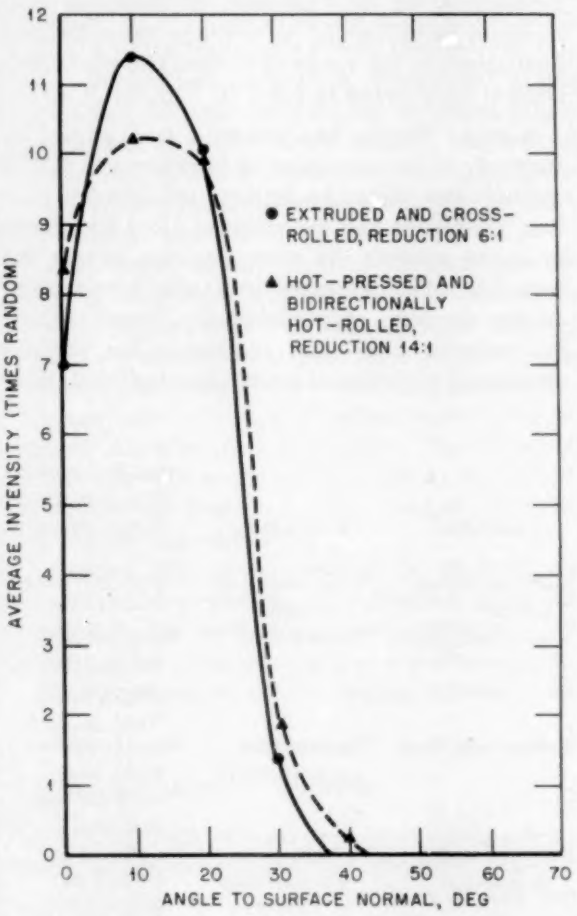
AVERAGE INTENSITY (TIMES RANDOM)
ANGLE TO SURFACE NORMAL, DEG
● EXTRUDED AND CROSS-ROLLED, REDUCTION 6:1
▲ HOT-PRESSED AND BIDIRECTIONALLY HOT-ROLLED, REDUCTION 14:1

Fig. 6 — Basal-pole distribution with respect to surface normal for comparison of textures by extrusion, cross rolling, and hot-press bidirectional rolling. Nuclear Metals data.[1]

the basal-pole reflections. (These intensities are proportional to the fraction of grains having that particular orientation.) The intensities are relative and are given in terms of the intensity for the corresponding angle from a randomly orientated specimen. Thus, for the fabrication procedures indicated in the figure, the major fractions of the crystals are oriented so their basal planes are nearly parallel to the plane of the sheet. Beryllium sheet with this texture is called "basal-plane layered." Such material, produced with a grain size of about 0.025 mm by extrusion and cross rolling, has a tensile elongation of from 30 to 40 per cent in the plane of the sheet. Beryllium with about the same grain size and texture, produced by hot pressing and bidirectional rolling, has a tensile elongation of about 25 per cent in the plane of the sheet. Basal-plane-layered beryllium does not reduce in thickness when plastically deformed in tension and is assumed to have no ductility in the direction normal to the sheet surface. The effect of grain size on strength in basal-plane-layered beryllium is shown in Fig. 7. The data show the

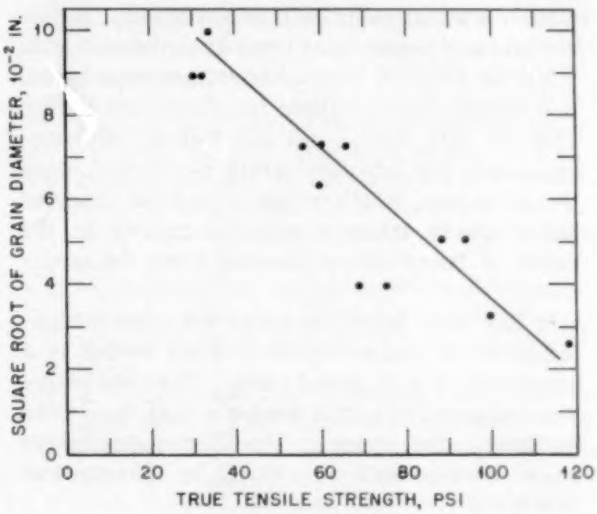

Fig. 7 — True tensile strength in basal-plane-layered beryllium related to grain diameter. Nuclear Metals data.[1]

pronounced effect refining the grain size can have on the ultimate tensile strength.

Another investigation which ties in with this work is a study of the factors which must be considered in making beryllium sheet with reproducible properties.[2] The factors which appear to be important are preferred grain orientation, grain size, fabrication temperature, and oxygen content (as it affects grain size).

Kells, Holden, and Whitman[3] have reported briefly on the preparation of a beryllium amalgam by the electrolysis of a $BeCl_2$-NaCl bath over a mercury cathode at 300 to 350°C. It is possible that the technique might be adapted to produce ultrafine beryllium powder, which, when pressed, extruded, and rolled, might result in extremely fine-grained basal-plane-layered beryllium. The extrapolation of Fig. 7 to finer

grain size indicates that this approach should be pursued to its ultimate conclusion. (It is interesting to note that the electrolysis of iron into a molten mercury cathode has been used to produce ultrafine iron particles 150 to 200 A in diameter.)

Other work at Nuclear Metals is concerned with efforts to confirm or refute the existence of a solid-state phase change in beryllium at temperatures near the melting point.[2] If such a transformation exists, it might be utilized in producing a fine-grained structure. On heating a metal through its solid-state transformation point, the conditions of nucleation and growth are often such that grain refinement occurs. In this respect one experiment tried at Nuclear Metals might be noted. A strip of beryllium was heated in a temperature gradient (running from 1275 to 1288°F). The hotter end was melted. Microexamination did not show grain refinement along the specimen, which might have been expected had a phase transformation occurred in the range of temperature existing along the specimen.

It has been shown in other work that a high-temperature phase transformation exists in a beryllium–8 at.% nickel alloy.[4] Thermal analysis and metallographic analysis have been used to detect this change. The high-temperature phase decomposes at 1065°C by a eutectoid reaction.

Thermal analyses are being made on dilute nickel alloys of beryllium in further efforts to delineate the phase constitution of beryllium per se.[5] Diffusion couples of beryllium/beryllium–6 at.% nickel and beryllium/beryllium–2 at.% iron are also being studied.[5] Diffusion couples indicate phase constitution since, in the diffusion region, the various phases existing at the diffusion temperature are developed.

Work at Nuclear Metals on the high-temperature properties of beryllium containing small amounts of a dispersed intermetallic phase continues.[2,6] The systems beryllium-SiO_2, -Fe_2O_3, -Be_2C, and -Al_2O_3 are receiving attention in this work. No new data are reported since the last issue of this Review. The observation was made, however, that Be_2C was more effective than SiO_2 in increasing the stress-rupture properties at 1200 to 1350°F when comparison was made at equivalent volumetric dispersions of the intermetallic phase. On the same basis it was also noted that Al_2O_3 was considered to be more effective as a strengthener than SiO_2.

In connection with high-temperature alloys, beryllium-BeO compositions are of promise. The linear thermal expansion of four beryllium-BeO compositions has been reported in an Oak Ridge publication.[7] Over the range 100 to 900°C, the coefficient of linear thermal expansion is insensitive to BeO content, at least for BeO contents up to 3 wt.%. An average value for this coefficient in the range of temperature and BeO content considered is 1.8×10^{-5} in./(in.)(°C).

Nuclear Metals has issued a final report on its study of the corrosion of beryllium in 600°F water.[8] The variables studied included fabrication procedure and the effect of alloy additions. In these studies the time elapsing before the inception of accelerated local attack was taken as the measure of performance. Some idea of the relative corrosion resistance for various conditions is indicated in the following tabulation:

Material	Fabrication	Time to inception of accelerated local attack
QMV beryllium powder	Hot-pressed or extruded	140 to 160 days
Pebble beryllium	Vacuum cast	Complete disentegration in less than 2 days
Pebble beryllium	Vacuum cast and extruded	Some improvement over vacuum-cast material
Beryllium–0.1 at.% nickel	Vacuum cast and extruded at 1950°F; extrusion ratio, 144 : 1	No sign of accelerated attack after 280 days

The corrosion resistance appears to be exceedingly sensitive to the fabrication variables, and it is apparent that much work needs to be done in developing materials with reproducible corrosion properties.

A study is being conducted at Nuclear Metals on the effects produced by helium generated in beryllium during the irradiation of the metal.[2] Tests will be conducted at 500°C. The extent of any swelling will be noted, and on completion of the tests the samples will be melted and the amount of helium evolved will be determined.

(A. J. Griest)

Solid Hydrides

Zirconium Hydride

Battelle is measuring the isothermal diffusion rates of hydrogen in zirconium and zirconium hydride[9] in an effort to obtain information which will aid in the interpretation of the experimentally determined migration patterns. It was found that the diffusion rate for hydrogen in beta zirconium is of the order of 10^{-4} cm^2/sec at 600 to 700°C. The diffusion rate for hydrogen in delta zirconium hydride was found to be 1.1×10^{-7} cm^2/sec at 400°C.

Oak Ridge[10] is investigating the crystal structure of zirconium hydride and other transition metal hydrides by X-ray diffraction at both high and low temperatures. They have shown that the crystal structure of the higher hydrides of zirconium are cubic close-packed with hydrogen atoms in tetrahedral interstices. The tetragonal distortion in the higher hydrides at room temperature was observed. A mechanism of hydride formation was postulated.

Denver Research Institute is studying the dissociation pressures of zirconium alloy hydrides.[11] No data have been reported yet. Alloying constituents used are lanthanum, niobium, praseodymium, scandium, titanium, and vanadium.

Zirconium-Uranium Hydride

The hydride of a zirconium-uranium alloy is still being considered for possible use as a combination fuel moderator. Knolls and Battelle[12] are measuring the solubility of hydrogen in these alloys. The latter work shows that the dissociation pressure of the hydride of a 1 wt.% uranium alloy does not differ noticeably from the dissociation pressure of the hydride of pure zirconium. Knolls is also studying the migration of hydrogen in zirconium-uranium alloys.

Battelle[12] is preparing a 1 wt.% enriched uranium-zirconium alloy hydrided to a hydrogen-zirconium atomic ratio of 1.6 for irradiation at 1200 and 1500°F. (J. B. Vetrano)

References

1. J. Greenspan, Ductility in Beryllium Related to Grain Orientation and Grain Size, NMI-1174, Aug. 9, 1957. (Unclassified AEC report.)
2. Fundamental and Applied Research and Development in Metallurgy, Progress Report for August 1957, NMI-2061, Sept. 26, 1957. (Secret AEC report.)
3. M. C. Kells, R. B. Holden, and C. S. Whitman, The Preparation of Beryllium Amalgam, *Journal of the American Chemical Society*, 79: 3925 (July 1957).
4. J. T. Norton, R. E. Ogilvie, and A. R. Kaufmann, Physical Metallurgy of Uncommon Metals, AECU-3556, May 15, 1957. (Unclassified AEC report.)
5. Fundamental and Applied Research and Development in Metallurgy, Progress Report for July 1957, NMI-2060, Aug. 8, 1957. (Secret AEC report.)
6. Fundamental and Applied Research and Development in Metallurgy, Progress Report for April 1957, NMI-2057, May 15, 1957. (Secret AEC report.)
7. J. E. Barton and S. D. Fulkerson, Linear Thermal Expansion of Four Different Compositions of Be and BeO, CF-56-11-59, Nov. 7, 1956. (Unclassified AEC report.)
8. D. S. Kneppel, Corrosion of Beryllium in 600°F Water, NMI-1190, Sept. 10, 1957. (Unclassified AEC report.)
9. R. W. Dayton and C. R. Tipton, Jr., Progress Relating to Civilian Applications During October 1957, BMI-1232, Nov. 1, 1957. (Unclassified AEC report.)
10. J. H. Frye et al., Oak Ridge National Laboratory, Dec. 13, 1957. (Unpublished.)
11. R. L. Beck, Denver Research Institute. (Unpublished.)
12. R. W. Dayton and C. R. Tipton, Jr., Progress Relating to Civilian Applications During November 1957, BMI-1238, Dec. 1, 1957. (Unclassified AEC report.)

Control-rod Alloys

Hafnium

The high cost of crystal-bar hafnium has somewhat curtailed its use as a control-rod material. However, the Bureau of Mines reports[1] that recent developments in the Kroll process technique for producing hafnium, using sodium-magnesium reductants, results in high-purity sponge material amenable to hot- and cold-fabricating techniques. Previous Kroll process hafnium could not be fabricated because of impurities.

Bettis has found that sponge-hafnium material is harder, stronger, and less ductile and has greater notch sensitivity than crystal-bar hafnium. This is due to the slightly higher impurity content in the sponge hafnium. No differences between the materials were noted in density, corrosion resistance, or weldability.

Silver-base Alloys

Bettis[2] irradiated a silver–15 wt.% indium–4.8 wt.% cadmium alloy to a maximum exposure of 1.44×10^{21} nvt thermal. Hardness of the specimen with greatest exposure increased from 56 to 72 DPH, whereas the specimen receiving the lowest exposure (0.33×10^{21} nvt) increased in hardness to 94 DPH. Yield strength increased from 8400 to 13,650 psi for the highest exposure sample and to 27,900 psi for the lowest exposure sample. There were no changes in the ultimate strengths. The strengthening effects probably resulted from formation of tin by transmutation from indium. Highest exposure samples showed less increase in strength because high temperatures during irradiation partially annealed out effects of strengthening. There were no dimensional or metallographic changes.

A silver–15 wt.% indium–5 wt.% cadmium alloy corrosion tested for 224 days in static neutral water at 500 to 650°F showed corrosion rates of 0.11 to 0.18 mil per year.[3] Irradiated specimens had the same corrosion rates as unirradiated specimens after 28 days in static neutral water at 650°F.

In a dynamic-loop corrosion test, a silver–14.8 wt.% indium–5.6 wt.% cadmium alloy was exposed to 4×10^{19} nvt thermal in 510°F, dynamic (19 fps), high pH (9.5 to 10.5 with KOH) water.[2] After 21 days the samples displayed zero corrosion rates. This was probably due to the formation of tin during irradiation since tin is known to improve the corrosion resistance of silver-indium-cadmium alloys.

Bolted assemblies of silver–15 wt.% indium–5 wt.% cadmium in contact with Zircaloy-2 and type 304 stainless steel showed no evidence of contact-line corrosion after 750 hr in 680°F water. Corrosion rates when calculated on the basis of exposed area were found to be comparable to corrosion rates of individual samples.

Creep-test data[2] obtained at Bettis for a wrought silver–15 wt.% indium–5 wt.% cadmium alloy indicate that a stress of 135 psi at 550°F results in a creep rate of 1 per cent in 10,000 hr. If the dead-load stress in service is 43 psi, the actual creep at 550°F for a life of 50,000 hr will result in about 0.5 per cent strain. An extruded and annealed (2 hr at 650°C) powder alloy appears to have a much higher creep strength than the wrought alloy.[4] At 4870 psi and 600°F, the wrought alloy had a minimum creep rate of 1.5×10^{-2} in./(in.)(hr) and ruptured in 13 hr, whereas the powder alloy at 5000 psi and 600°F is showing a minimum creep rate of 5.77×10^{-6} in./(in.)(hr) after 600 hr.

Knolls is attempting to improve the mechanical properties of the silver-indium-cadmium alloys through addition of platinum, palladium, rhodium, iridium, ruthenium, arsenic, antimony, and tin in amounts up to 1 wt.%. Additions of platinum in excess of 0.1 wt.% were found to increase the strength considerably. However, the previously reported increase in yield strength from 13,100 to 34,800 psi for an alloy with a 1.0 wt.% platinum addition was found to be high. Work hardening of the specimen during a forging operation is believed to have led to the high

strength results. Iridium has been found to decrease the strength of the alloy.

Silver-iridium-cadmium-tin alloys, made up to simulate material which has undergone irradiation, have significantly greater strength than the base alloy.[5] A silver–15 wt.% iridium–5 wt.% cadmium alloy extruded and heat-treated ½ hr at 400°C and air-cooled had a yield strength of 17,570 psi, whereas a similarly treated silver–15 wt.% indium–3.5 wt.% cadmium–1.5 wt.% tin alloy had a yield strength of 25,230 psi. Aging these alloys produced a marked drop in strength. The base alloy had yield strengths of 9500 psi after aging at 600°F for 720 hr and 7700 psi after 1440 hr at 600°F. Drop in yield strength of the alloy with the tin addition was not as great, the yield strength being 23,000 psi after 720 hr and 21,020 psi after 1440 hr.

Boron - Stainless Steel

Bettis[6] investigated austenitic stainless-steel alloys containing up to 3 per cent boron for possible use as a control-rod material. Irradiation of the alloys resulted in a large decrease in impact strength. Table III-1 illustrates the effect of irradiation on impact strength of B^{10}–stainless-steel alloys. Hafnium and stainless steel are also listed for comparison. Cladding the boron–stainless-steel core with austenitic stainless steel improved the impact strength somewhat, but the material still fell short of specifications. (V. W. Storhok)

Table III-1 RESULTS OF IMPACT TESTS ON IRRADIATED B^{10}–STAINLESS-STEEL ALLOYS (BETTIS DATA[6])

Material	Condition	Testing temp., °F	Non-irradiated Izod, ft-lb	Irradiated Izod, ft-lb	Exposure, nvt	
					Thermal	Fast
Hafnium*	Annealed	RT	2.38	1.14	2.7×10^{20}	3×10^{18}
Hafnium	Annealed	600	8.83†	8.16†	2.7×10^{20}	3×10^{18}
Type 347 stainless steel‡	Annealed	RT	15.90†	15.60†	3×10^{20}	6×10^{19}
0.5 wt.% B^{10}–stainless steel‡	Annealed	RT	9.52†	1.48	3×10^{20}	3×10^{19}
0.5 wt.% B^{10}–stainless steel	Annealed	600	8.43†	1.48	3×10^{20}	3×10^{19}
0.5 wt.% B^{10}–stainless steel	Postirradiation heat-treated§	RT	9.52†	0.52	6.6×10^{20}	1.5×10^{20}
0.5 wt.% B^{10}–stainless steel	Postirradiation heat-treated	600	8.43†	0.34	6.6×10^{20}	1.5×10^{20}
0.85 wt.% B^{10}–stainless steel	Annealed	RT	5.67	0.24	9×10^{20}	1.8×10^{20}
0.85 wt.% B^{10}–stainless steel	Annealed	600	5.70	0.18	9×10^{20}	1.8×10^{20}
0.85 wt.% B^{10}–stainless steel	Postirradiation heat-treated	RT	6.05	0.24	9×10^{20}	2.1×10^{20}
0.85 wt.% B^{10}–stainless steel	Postirradiation heat-treated	600	5.93	0.36	9×10^{20}	2.1×10^{20}
0.85 wt.% B^{10}–stainless steel	Nitrogen quenched	RT	5.77	0.36	6.6×10^{20}	1.8×10^{20}
0.85 wt.% B^{10}–stainless steel	Nitrogen quenched	600	6.62	0.48	6.6×10^{20}	6×10^{19}

* Hafnium annealed at 1600°F and furnace-cooled.
† Bent; did not fracture.
‡ Stainless steel and B^{10}–stainless steel annealed at 1950°F, 1 hr and furnace-cooled.
§ Postirradiation heat-treatment: 24 hr at 750°F.

Dispersion-control Materials

Compartmented type control rods continue to be investigated at Bettis. A series of specimens

containing compartments filled with B_4C (enriched boron, approximately 90 per cent B^{10}) and clad with Zircaloy-2 is being completed. A second type of compartmented rod contains boron pins which are made by extruding boron powder mixed with a binder and subsequently sintering the pins in hydrogen to remove the binder. A rod was prepared in this manner to be used for shock testing; however, local swelling occurred at 700°C, probably due to residual binder or adsorbed hydrogen. Additional specimens are being prepared. Battelle has been corrosion testing irradiated nondefected single-compartment specimens containing TiB_2^{10}, B^{10}, and $B_4^{10}C$ powders. Examination revealed no defects after exposure to 500°F water for 2500 hr. The TiB_2^{10} specimens showed a slight enlargement opposite the weld, and the B^{10} specimen showed surface pitting near the edge, but none of the specimens were enlarged over the boron-containing compartment. The amounts of helium released are being determined, but measurements have not been completed.

B_4C strips are being investigated by Knolls. The two types of strips being studied are B_4C depleted to 3 wt.% B^{10} and fabricated to 60 per cent of theoretical density and 11 wt.% natural B_4C dispersed in Al_2O_3 and fabricated to 60 per cent of theoretical density. Specimens will be placed in capsules pressurized to 1800 psi and irradiated in the MTR at 650°F maximum temperature under steady-state conditions.

Radiation effects on various boron-containing powders are being studied at Battelle. Postirradiation tests being conducted include X-ray diffraction, metallographic examination, particle-size determination, helium analysis after heat-treatment at a series of temperatures, high-temperature water-corrosion tests, and analysis for total lithium and helium retained in the powder. ZrB_2 powder which has been irradiated to a calculated burn-up of greater than 80 wt.% B^{10} is being examined. Preliminary analytical results show that 0.5 per cent of the calculated helium produced was contained in the capsule gas. Actual burn-ups will be determined from cobalt dosimeters enclosed in the capsule and by lithium and helium analysis of the powder. Other powders being investigated include HfB_2, B_4C, partially enriched HfB_2, EuB_6, and CaB_6.

A report published by Knolls[7] contains a discussion of the advantages of using dispersed boron control materials rather than boron alloys. Calculations are made to determine the effect of particle size and loading on the amount of undamaged matrix remaining after irradiation. Results of these calculations are qualitatively compared to actual results obtained on irradiation specimens at Knolls and other laboratories. As would be predicted, the dispersions show improved resistance to irradiation when compared to the alloys.

Work with dispersions of rare-earth oxides in metallic matrices is in progress at Oak Ridge.[8] Fabrication procedures and mechanical-property data are being obtained for Inconel-clad tubular control rods which contain a core of 30 wt.% Lindsey oxide (mixture of Sm_2O_3, Gd_2O_3, and small amounts of other rare-earth oxides) dispersed in nickel. At 1500°F the core material showed no appreciable ductility, supposedly because of stringering and agglomeration of the oxide particles. Inconel-clad extruded specimens cracked badly during cooling. At 1500°F two tensile specimens showed elongations of 5 and 2 per cent, respectively, compared to less than 0.1 per cent for the core specimens. In addition Oak Ridge is developing a dispersion of 30 wt.% Eu_2O_3 in an iron-base material as a substitute for a control rod of 3 wt.% B^{10} dispersed in iron. The preliminary work was carried out with Lindsey oxide No. 921 which was agglomerated by firing at 1700°C, then crushed to −44 μ size, mixed with −44 μ stainless-steel picture-frame pack, and hot-rolled at 1150°C to a total reduction of 91 per cent. Although the work with this Sm_2O_3-Gd_2O_3

Table III-2 EFFECT OF MATRIX MATERIAL, SINTERING TEMPERATURE, AND SINTERING TIME ON THE VOLUME CHANGE OF EUROPIUM OXIDE DISPERSIONS (OAK RIDGE DATA[8])

Matrix material	Sintering temp., °C	Sintering time, °C	Volume change, %
Type 302B stainless steel	1230	1.5	+6.71
	1120	1.5	+6.17
Type 304 stainless steel	1230	1.5	+6.22
Electrolytic iron	1150	1.5	−2.13
Nickel	1150	1.5	−1.52
Chromium (0.6 wt.% silicon)	1150	1.5	+2.15
Silicon	1200	1.5	+5.86
Elemental type 304 stainless	1200	1.5	+0.33
steel (<1 wt.% silicon)	1175	1.5	+0.00
Elemental type 304 stainless	1200	1.5	−4.43
steel (<0.2 wt.% silicon)	1200	1.25	−0.81

(G. W. Cunningham)

mixture gave good results, Oak Ridge indicates that a reaction takes place when Eu_2O_3 is dispersed in stainless steel. An electron micrograph shows a reaction zone between adjacent Eu_2O_3 and stainless type 302B particles. Also an increase in volume, rather than a shrinkage, occurred when the dispersion was sintered. Based on a series of sintering tests, it is stated that the silicon content of the matrix powders is important in determining the extent of reaction. As shown in Table III-2, reaction is indicated with silicon and those powders which contain high silicon contents; however, no explanation is given as to why the high-silicon stainless powder reacts more than the pure silicon. Also the data are not corrected for expected differences in shrinkage of the different matrices when Eu_2O_3 is not present. Nevertheless, in general, some shrinkage would be expected in all the materials.

References

1. H. Kato, R. A. Beall, H. P. Holmes, F. E. Block, and G. C. Ware, U. S. Bureau of Mines, Oct. 15, 1957. (Unpublished.)
2. I. Cohen, Westinghouse Atomic Power Division, Oct. 11, 1957. (Unpublished.)
3. Pressurized Water Reactor Project, Technical Progress Report, WAPD-MRP-70, Oct. 23, 1957. (Unclassified AEC report.)
4. I. Cohen, Westinghouse Atomic Power Division, December 1957. (Unpublished.)
5. D. N. Dunning, Knolls Atomic Power Laboratory, Dec. 18, 1957. (Unpublished.)
6. L. B. Prus, E. S. Byron, and J. F. Thompson, Westinghouse Atomic Power Division, May 13, 1957. (Unpublished.)
7. D. W. White, A. P. Beard, and A. H. Willis, Irradiation Behavior of Dispersion Materials, KAPL-P-1849, Nov. 22, 1957. (Unclassified AEC report.)
8. Oak Ridge National Laboratory, Dec. 13, 1957. (Unpublished.)

Corrosion

Corrosion by Liquid Metals and Fused Salts

A recent annual progress report[1] issued by the Metallurgy Division at Oak Ridge includes information from a myriad of corrosion tests in several high-temperature baths. Many materials and parameters were evaluated in experiments ranging from static screening exposures to exposures in forced-convection polythermal flow-loop systems. The several topics from this report summarized below illustrate the variety of the activities at this laboratory; the particular ones chosen for inclusion here are either fairly new in scope or serve to shed light on old, somewhat controversial issues in the high-temperature-liquids corrosion field.

1. *Effect of Grain Size on Attack in the Inconel–Fluoride Salt (50 Mole % NaF, 46 Mole % ZrF_4, 4 Mole % UF_4) System.* Results of a 1600°F peak-temperature pumping-loop experiment with the above combination indicate a good possibility for accentuated (perhaps by a factor of 2) grain-boundary attack with coarse-grained Inconel. The Inconel employed in this case was annealed before the experiment for 2 hr at 1940°F in hydrogen. This treatment produced grains varying in size from ASTM No. 5 to nearly No. 1; normally, grain size in Inconel is in the ASTM 4 to 8 range.

This general result demonstrates that containment-material grain size should be recognized as a corrosion-controlling factor when dealing with a corrosion process in which grain-boundary penetrations are important. The corrosion of Inconel by molten fluoride salts is characterized by a leaching of chromium which leads to the formation of voids at grain boundaries.

2. *Effectiveness of Oxide Formers in Inhibiting Mass Transfer in the Inconel-Sodium System.* Three 1500°F peak-temperature flow loops were operated in this series. Oxide formers added to individual systems were, respectively:

1. A 2.27 wt. % concentration of magnesium obtained by a pre-exposure of the sodium charge to magnesium chips.
2. Crystal-bar titanium rod in the hot leg.
3. Crystal-bar zirconium rod in the hot leg.

As a whole, during 1000-hr exposures, the getters had no marked influence either on the corrosion (about 1 mil in the hot zone) or on the quantity of cold-zone deposit. Before-and-after oxygen levels for these systems were not reported. If the original levels were low, it is not surprising that the getters failed to produce a significant change in the corrosion situation. Based on past experience pertaining to the role of oxygen in the sodium corrosion process, it might be expected, if the metal-oxygen levels were high, that getters such as were used would result in measurably decreased corrosion during a long exposure.

3. *Effect of Cold-trap Temperature on Mass Transfer in Inconel-NaK (56 Wt. % Sodium–44 Wt. % Potassium) Forced-circulation Loops.* Cold traps in 1500°F peak-temperature NaK loops were operated at peak temperatures of 100, 300, 600, and 800°F; the purpose here was to control the oxide level in the test charges by means of the decrease in the solubility of sodium oxide in sodium with increased trap temperature. Weight determinations of cold-zone mass-transfer deposits removed from the various systems after 1000 hr of operation yielded the expected trend of increased deposit with increased cold-trap temperature (actual deposit thicknesses ranged from 7 to 20 mils). The composition of deposits in all cases was approximately 90 wt. % nickel and 10 wt. % chromium.

4. *Effect of Flow Velocity on Mass Transfer in Inconel-Sodium Loops.* Two 1500°F peak-temperature flow loops were operated with sodium circulating at different velocities to check the effect of this parameter on mass-transfer accumulations. Specific results after 1000-hr runs are listed on following page.

Loop flow rate, gal/min	Weight of deposit, g	Thickness of deposit, mils
1½	10.4	12
3	14	22

These data suggest that the higher the flow rate the greater the corrosion. This is the trend that might be predicted for a solubility-dependent corrosion process occurring in a polythermal flow system.

5. *Evaluation of Several Alloys for Service with High-temperature Sodium.* Polythermal flow loops fabricated of several alloys were operated for 1000 hr to evaluate compatibility with high-temperature sodium. Pertinent results for 1500°F peak-temperature experiments are as follows:

1. Loops fabricated from types 347 and 304 stainless steel displayed less mass transfer than would be expected from comparable Inconel loops. Surface pitting to 2 mils occurred in the hot zones of the stainless-steel systems.

2. A loop fabricated of Incoloy (iron–34 wt. % nickel–20 wt. % chromium) displayed both hot-zone intergranular corrosion (about 2 mils) and cold-zone deposits similar to those in Inconel systems. The deposits contained about equal amounts of nickel and chromium, along with a small quantity of iron.

3. Hastelloy B loops contained somewhat more cold-zone deposits than would be expected with Inconel; nickel was the principal deposit constituent. Hot-zone attack was of the order of 1½ mils.

4. Hastelloy W loops contained about 17 per cent more mass transfer than did the Hastelloy B systems. Hot-zone areas were heavily attacked to 1½ mils.

One experiment was conducted using 1300°F peak-temperature sodium in a Hastelloy B system. General corrosion here was comparable to that for similar Inconel systems. It would appear that attack in sodium-containing Hastelloy B systems increases more rapidly with temperature level than is the case for Inconel systems.

Jepson[2] reports that niobium has excellent resistance to pure molten sodium and sodium-potassium alloys at 600°C (less than 1 mil attack per year), but oxygen in the coolant increases the rate of attack and must be maintained at low levels.

6. *Behavior of Tantalum in Sodium.* Flow-loop studies have been conducted at Battelle[3] to evaluate the behavior of tantalum (from commercial sources) specimens in contact with high-temperature high-purity sodium; this investigation furnished information to the LAMPRE I (a sodium-cooled fast reactor featuring tantalum as the molten-plutonium-alloy container material) development program at Los Alamos Scientific Laboratory. The exposures were made in small polythermal forced-convection flow-loop systems, each fabricated of type 316 stainless steel and equipped with a cold trap, a zirconium-foil-filled gettering trap, and a plugging indicator for control and monitoring of sodium-oxygen levels. Conditions for the majority of experiments were as follows: peak sodium temperature, 1200°F (the primary specimen exposure temperature); nominal fluid-temperature cycle, 500°F; oxygen level in sodium, from <10 to 80 ppm; and test period, from 200 to 1200 hr.

The general trends established from the tantalum-sodium research are listed below; they leave little doubt about the excellence of tantalum for sodium containment in the 1200°F range.

1. Specimen weight losses were fairly low; the maximum loss recorded represents only about 1 mil of metal removed from the exposed surfaces per year. There was, however, a discernible effect of sodium-oxygen level on tantalum weight loss; as might be expected, higher oxygen levels led to increased removal of metal.

2. Although the nitrogen content of the tantalum specimens was not affected by sodium exposure, their oxygen content, which originally ranged from about 100 to about 300 ppm, was consistently lowered to the neighborhood of 75 ppm. This removal of oxygen from tantalum by sodium could not have been predicted from available thermodynamic information except for the case of very pure sodium, containing oxygen in the 1 ppm range, for example.

3. Metallographic examinations of exposed tantalum specimens indicated that intergranular attack had not occurred. The only effect detected was a slight roughening of the exposed surfaces.

4. Posttest inspections of loop systems thus far completed have not yielded evidence of the

formation of cold-zone mass-transfer deposits of significant magnitude.

7. *Solubility of Carbon in Sodium.* The carbon content of high-temperature containment materials can be altered by exposure to molten sodium. The solubility of carbon in sodium, which is basic to this situation, has recently been determined at Knolls.[4] For the experimental conditions employed the following equations can be used to relate solubility, S, in ppm to bath temperature, T, in degrees centigrade.

$$\ln S = 4.96 - 6.21 \times 10^2/T \text{ at } 0.004 \text{ wt.\% oxide content}$$

$$\ln S = 5.61 - 3.76 \times 10^2/T \text{ at } 0.026 \text{ wt.\% oxide content}$$

The variation represented is 32 to 74 ppm over the test-temperature range of 147 to 700°C at the 0.004 wt. % oxide level; at the 0.026 wt. % level, the corresponding variation is from 112 to 186 ppm.

8. *Corrosion by Molten Heavy Metals.* The Coolant Chemistry Laboratory at Knolls recently investigated[5] the behavior of the Chromel-Alumel combination in the following five heavy-metal baths held at 1000°F: lead, bismuth, bismuth–5 wt. % lead, bismuth–45 wt. % lead, and tin. Both materials suffered severe attack. In the case of Alumel, intergranular penetration was prominent; Chromel also displayed this kind of attack and was, in addition, badly embrittled. The investigation also covered the compatibility of an 8 wt. % uranium-zirconium alloy in the above media. This alloy was consistently damaged through the formation of intermetallic compounds.

9. *Lithium-corrosion Bibliographies.* Very useful lists of references pertaining to corrosion by molten lithium and related subjects have been issued recently.[6,7] The list compiled by Hoffman and Johnson was in connection with a Lithium Symposium held at Oak Ridge Aug. 8–9, 1957. (J. H. Stang)

Zirconium in Oxidizing Media

Although the air oxidation of zirconium and its alloys, crevice corrosion, hydrogen pickup during corrosion testing, and corrosion quality-control tests are being studied at several laboratories, the stringer type corrosion phenomenon observed for Zircaloy compositions continues to receive major attention. Efforts to date, directed toward determining the relation between fabrication procedures and stringer corrosion and the mechanisms which promote stringer formation, have not established the exact nature of the stringers or a successful treatment to salvage material already committed to manufacture. Studies at Bettis,[8,9] however, have indicated two important facts:

1. Vacuum-melted zirconium alloys are less susceptible to stringer corrosion than are inert-atmosphere-melted alloys.

2. Fabrication and heat-treatment history influence corrosion behavior in high-temperature water and steam; e.g., available records indicate forged materials are more resistant than bloomed materials. In addition, annealing treatments at 1800°F for 4 to 8 hr, followed by an air quench, improve corrosion properties. Some benefit also was observed for a 1700°F treatment, whereas 1500 and 1600°F anneals did not result in any improvement. This change in corrosion behavior is explained on the basis of the solution and redistribution of the intermetallic compound particles in the matrix.

A comprehensive review, comparison, and critique of the zirconium-water reaction rate experiments of the past several years has been published by Bettis.[10] The general conclusion is that fair agreement of experimental results exists for widely different experimental techniques, and recommendations are made as to which data should be utilized in analytical studies.

The development of an accelerated test to detect regions of inferior corrosion resistance of Zircaloy materials also has been the subject of investigation at Bettis. Current results have indicated that an electrolytic technique, in which Zircaloy is made the anode in an ammonium diborate electrolyte, could be used with a fair degree of reliability to differentiate between stringered and unstringered material.

Crevice corrosion has been the subject of investigation at Knolls. Simulated crevices fabricated using sandwich type specimens of Zircaloy-3 have been used to study the effect of various washing techniques after pickling on corrosion behavior. Barrier voltage measurements, after 3 to 14 days of exposure in steam, indicate that a protective film was beginning to form under white corrosion product developed

in samples allowed to dry after pickling. This appears to suggest that crevice corrosion may not be expected to continue to a dangerous extent.

Studies which have contributed to an understanding of the oxidation and scaling behavior of zirconium and its alloys are being conducted at Case Institute of Technology.[11] In these studies the scaling behavior of binary and ternary zirconium-base materials containing a maximum alloy content of 5 wt.% was determined in air at temperatures up to 1800°F. Of the 23 elements investigated, only nickel or copper additions significantly reduced scaling of unalloyed zirconium. Ternary zirconium-base alloys, in general, show little or no improvement in scaling behavior over that exhibited by the binary alloys.

Aqueous Corrosion of Aluminum Alloys

It has been demonstrated that aluminum can be made resistant to high-temperature water by small additions of nickel, iron, and copper. For optimum corrosion resistance, however, the second-phase particles of these alloys must be small and evenly distributed. In the presence of an adequate concentration of the second phase, the attack in water at 400°F and higher changes from localized penetration at grain boundaries and blister formation to the more desirable uniform over-all attack.

The mechanisms and kinetics of the aqueous corrosion of these alloys have been reported by Troutner of Hanford[12] and by Krenz of Chalk River.[13] In general, the data reported are in good agreement and indicate the following:

1. The corrosion product formed during the aqueous corrosion of aluminum consists of a thin, compact barrier film adjacent to the metal and a thicker and more permeable bulk film.
2. The barrier film is amorphous, whereas the bulk film is composed of a crystalline-hydrated oxide.
3. The corrosion process is controlled by the bulk film and not the barrier film.
4. The composition of the water affects the corrosion rate by altering the solubility and composition of the bulk film, whereas radiation and heat flux do not appear to alter corrosion behavior.
5. The onset of intergranular attack appears to be related to crystallization of the barrier film. The bulk film does not control the rate of intergranular attack.
6. The effect of alloy additions is manifested in the base metal and/or barrier film and not in the bulk film.

Probably the greatest obstacle to the use of aluminum-nickel alloys in their present state of development is the friability of the corrosion film. Coupled with this are the relatively poor mechanical properties of the alloys at elevated temperatures. In cooperation with the Aluminum Alloy Task Group's program to develop new aluminum-base alloys, corrosion studies are being conducted at several laboratories. Preliminary data reported by Hanford and Bettis[14] have shown that experimental alloys containing from 1.5 to 5 per cent nickel with additions of iron and copper or copper and titanium are more resistant to intergranular attack than the present M-388 and M-400 aluminum-nickel alloys.

Aqueous Corrosion of Stainless Steels

The use of type 304 stainless steel as a cladding material for fuel elements may be accompanied by corrosion problems under severe conditions of exposure. Work conducted at Knolls and Oak Ridge[15] has shown that annealing, brazing, and welding treatments during the fabrication of a fuel element may cause sufficient diffusion of carbon from the fuel core into the type 304L stainless-steel cladding to transform the material into a type 304 (normal carbon) alloy. Normally, sensitized 18-8 stainless steels are not subject to intergranular attack in high-temperature water. However, if such sensitized materials are treated for even a short time in an aggressive acid, some light surface intergranular attack occurs. Although this attack may not be detrimental, subsequent immersion in high-temperature water may lead to severe intergranular penetration. The latter is belived to result from entrapped acid in the surface grain boundaries.

Substitution of type 347 stainless steel for the low-carbon type 304L stainless-steel frame and cladding material results in a composite plate which, after fabrication, is not subject to intergranular attack. (W. K. Boyd)

Oxidation of Niobium and Molybdenum

Two studies have been published concerning oxidation principles of niobium and niobium alloys. An electron micrograph study conducted

at Oak Ridge[1] indicates that the transition from protective (parabolic type) scale formation to nonprotective (linear type) scale formation at 400°C is associated with the appearance of small blisters in the scale. The initial scale is adherent, and rippled blisters formed by accelerated local reaction ultimately result in the white porous scale associated with linear oxidation of niobium. The final linear rate is controlled by oxygen diffusion across a statistically constant adherent film. Battelle[16] work indicates that, at 1000 and 1200°C, the oxidation behavior of niobium alloys is controlled by size and valence of the alloying metal ions and by the chemical, physical, and mechanical properties of new scale phases formed during oxidation. In the low alloying range the addition-metal ions are soluble in Nb_2O_5. Smaller ions (chromium, vanadium, and molybdenum) contract the scale, promoting compact scale formation and decreased oxidation rates, and higher valence ions (Mo^{+6}) reduce diffusion rates through the compact scale. Larger ions (tantalum, tungsten, and zirconium) and lower valence ions (Zr^{+4}) have opposite effects and decrease oxidation resistance. With additions of more than 15 at.%, new scales are formed. These are nonprotective with molybdenum, vanadium, and chromium but are protective and stable with titanium and zirconium. Tenfold improvements in oxidation rate compared to pure niobium were possible by binary alloying.

Molybdenum can be protected from oxidation by sprayed coatings of aluminum-chromium-silicon, nickel-chromium-boron, and nickel-silicon-boron; electroplates of chromium and chromium-nickel; and claddings of pure nickel, according to a study completed at Climax Molybdenum Co.[17] The sprayed coatings had best oxidation resistance but only moderate erosion resistance at 1800°F. The electroplated and clad specimens showed good erosion resistance but lower oxidation resistance than the sprayed coatings. Nickel-base coatings are self-healing, forming $NiMoO_4$ at cladding defects. This oxide is protective, although it spalls from large areas on cooling. Protection at temperatures as high as 2600°F for at least 4 hr is possible with sprayed aluminum-chromium-silicon. These methods of protection are making possible the use of molybdenum in jet engines.[18]

(W. D. Klopp)

Corrosion of Nickel and Nickel-base Alloys

1. *Oxidizing Media.* Some of the effects of high-temperature oxidation on high-temperature high-strength nickel-base materials (Nimonic type alloys) have been qualitatively recognized as surface depletion of the more reactive ingredients (chromium, aluminum, and titanium) and surface fissuring of materials subjected to oxidation. Parfenov[19] has explained the occurrence of fissures in such materials as resulting from recrystallization in the surface regions of the metal as a result of alloy depletion. Recently, workers at the French National Office of Studies and Aeronautical Research[20] studied the effects of oxidation on Nimonic-80 and -95, among other alloys, and presented a theoretical analysis of the expected changes in mechanical properties of the alloys.

Regarding the oxidation resistance of specific materials, the National Bureau of Standards has a program in progress in which the oxidation resistance of various experimental alloys at elevated temperatures is being examined. Two alloys[21,22] studied to date are nickel-base Hastelloy R235 and Hastelloy W. Both these alloys follow the parabolic rate law, and activation energies for the oxidation reaction were calculated as 58,900 cal/mole for Hastelloy R235 and 57,200 cal/mole for Hastelloy W. (These activation energies have not been correlated with a particular oxidation mechanism but are intended only to show the temperature dependency of the oxidation reaction.) Direct comparison of these alloys and other heat-resistant materials will be made in a future report.

Work at Knolls has dealt with the corrosion of Inconel in water at 600°F to determine its suitability for a pressure vessel seal ring. Two-week exposures to ammoniated water containing hydrogen and to aerated water showed no corrosion in the hydrogen-containing water but showed a thin, nonadherent, yellow film in aerated water (quantitative attack was very slight, 0.4 mg/dm^2).

2. *Nitriding Media.* Experimentation by Trillat et al.[23] showed that at 300 to 390°F ammonia reacts with nickel, wherein nitrogen penetrates the lattice, causing expansion of the face-centered cubic nickel structure. Above 390°F nitrogen (from ammonia) transforms the lattice to a hexagonal close-packed structure corresponding to Ni_3N. Although the reported mecha-

nism is not necessarily a corrosion process, the possible effects of structural modification by the penetration of the environment make this worthy of mention.

Oxidation of Chromium and Chromium-base Alloys

Ames Laboratory[24] reported the results of corrosion tests in 570°F steam for exposure times up to 28 days. Alloys containing from 40 to 60 at. % chromium (balance vanadium or molybdenum) showed no significant corrosion. (Molybdenum-vanadium, tungsten-vanadium, and tungsten alloys were severely corroded by these conditions.) Oxidation at 930°F showed "little or no oxidation" of 60 wt. % chromium–40 wt. % (vanadium, molybdenum) alloys.

Radiation Effects on Cladding and Structural Materials

Basic Studies

Recent reference on the fundamentals of irradiation effects deals mainly with correlation of physical and crystal-lattice expansion and of electrical conductivity with motion of defects by annealing.

The work at the University of Illinois[25] on low-temperature deuteron irradiation of metals has shown reasonably good correlation of physical expansion with crystal-lattice expansion and electrical conductivity. The measurements of physical expansion of copper, made during irradiation with 8.5 Mev deuterons at 17°K, agree with prior lattice-expansion data, within the errors for both measurements. The concentration of defects calculated from the expansion gave 7.6×10^{-21} per deuteron per cm^2 or 6.4 per deuteron, which is about one-sixth the amount given by theory. The annealing of physical expansion follows that of lattice expansion and resistivity. From determination of activation energy,[26] Illinois workers conclude that the annealing process below 60°K is mainly one of movement of interstitials, with interstitials and vacancies occurring as close pairs. Assuming 5 ev for formation of a Frenkel defect, the energy was estimated as 5.4 cal/g/μohm-cm. By comparison, Overhauser[27] obtained 1.7 cal/g/μohm-cm from liquid nitrogen temperature to room temperature. Correcting for the 64 to 70 per cent recovery at liquid nitrogen temperature, the data would indicate a stored energy of 1.9 cal/g/μohm-cm as compared to Overhauser's data.

Willis and Smallman[28] have carried out a study which sheds light on the mechanism of radiation damage in ionic compounds. They reported extensive work on slow-neutron-irradiated lithium fluoride, wherein marked effects would be expected from the (n,α) reaction in Li^6. Linear crystal expansion was observed up to 1×10^{17} slow neutrons per cm^2; beyond this, expansion was nonlinear, with a maximum at 4×10^{17} and a decrease on further irradiation. Strain, as observed by X-ray diffraction broadening, started increasing at 1×10^{17} neutrons per cm^2 and was linear to 7.2×10^{18} neutrons per cm^2. They found an agglomeration of defects above 3×10^{17} neutrons per cm^2 as indicated by low-angle X-ray scattering. From the expansion the number of defects per (n,α) reaction was estimated at 1900. Thus the initial defects are of the Frenkel type, with agglomeration occurring at about 2 per cent defects. The defects anneal out between 400 and 500°C, but gas bubbles of 6 μ square cross section form at 700°C. The agglomeration of defects at higher irradiations would decrease the concentration of interstitials and centers of expansion. Therefore these results are essentially consistent with the early work of Binder and Sturm[29] at lower total flux and of Keating[30] at higher flux.

Hanford[31] has obtained additional data on annealing of neutron-irradiated molybdenum which indicates two processes. The first was completed around 200°C and accounted for less than one-half of the irradiation-induced damage. The crystal-lattice expansion correlated with hardness. (A. E. Austin)

Effects of Irradiation on Mechanical Properties

Further results of studies of the effects of irradiation on the properties of Zircaloy-2 have been reported by Hanford.[32] Irradiation to 1.4×10^{21} nvt (thermal flux) produced the following effects:

1. Developed yield point.
2. Increased yield strength approximately 60 per cent.
3. Increased ultimate tensile strength approximately 17 per cent.

4. Reduced total elongation ~ 35 per cent.

5. Flow curve exhibited region of low work hardening after yield, and strain-hardening exponent was lowered to nearly the same value as for cold-worked material.

When material was cold-worked 50 per cent prior to irradiation, the yield point did not develop, the yield strength increased 30 per cent, the ultimate tensile strength increased 17 per cent, and elongation was reduced 51 per cent. Annealing tests indicated that the yield point could be removed by annealing at 300°C after irradiation. Appreciable recovery as measured by yield strength required higher temperatures, as shown in Fig. 8. The data also show that the recovery of radiation damage occurs by a mechanism comparable to recovery from cold work. The activation energy for 50 per cent recovery of yield strength was calculated to be 49,200 cal/mole.

Further information[33] has been reported by Phillips on the effects of irradiation on various structural materials. Table IV-1 shows the results of tensile tests of irradiated specimens. Irradiated impact specimens are being tested.

The effects of irradiation on the postirradiation tensile properties of several magnesium alloys have been reported by Harwell.[34] Specimens were irradiated to doses of approximately

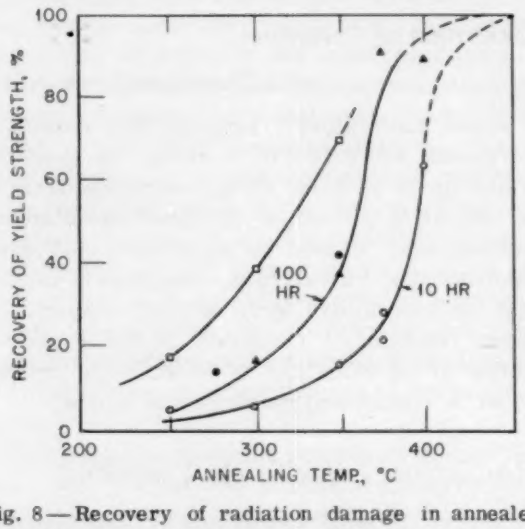

Fig. 8 — Recovery of radiation damage in annealed Zircaloy-2. □, 100-hr anneal of irradiated zirconium.[45] ●, 100-hr anneal of 15 per cent cold-worked Zircaloy.[46] ▲, 100-hr anneal of irradiated Zircaloy-2. ○, 10-hr yield of irradiated Zircaloy-2. Hanford data.[1]

Table IV-1 TENSILE-TEST RESULTS*

Material	Neutron irradiation: Days in MTR	Neutron irradiation: nvt thermal	nvt >1 Mev	Rockwell hardness	Tensile strength, psi: Ultimate	Tensile strength, psi: 0.2% offset yield	Elongation in 1 in., %	Reduction in area, %
1601 Croloy	0	0	0	B-83	76,500	57,800	36	71
	42	4.2×10^{20}	4.9×10^{19}	B-96	116,600	116,600		63
	84	6.1×10^{20}	7.8×10^{19}	B-95	108,600	108,600	14	60
Hastelloy X	0	0	0	B-87	112,500	49,400	52	52
	42	4.4×10^{20}	5.0×10^{19}	B-96	129,300	100,200	50	62
	84	1.4×10^{21}	1.8×10^{20}	B-99	130,700	104,000	43	64
	168	1.8×10^{21}	2.5×10^{20}	B-100	131,000	106,300	42	59
Inconel 702	0	0	0	B-82	94,900	42,600	67	68
	42	4.4×10^{20}	5.0×10^{19}	B-96	113,100	101,100	50	63
	84	1.4×10^{21}	1.8×10^{20}	B-100	121,500	120,300	41	64
	168	2.4×10^{21}	2.9×10^{20}	B-101	130,000	128,800	36	63
Inconel X (double aged)	0	0	0	C-27	170,100	103,200	28	36
	42	0.8×10^{20}	0.8×10^{19}	C-30	165,100	143,300	22	30
	84	1.2×10^{21}	1.6×10^{20}	C-30	161,300	158,600	14	43
Inconel X (single aged)	0	0	0	C-32	184,300	120,300	23	29
	42	0.8×10^{20}	0.8×10^{19}	C-34	172,600	154,500	18	32
	84	1.2×10^{21}	1.6×10^{20}	C-34	174,000	170,800	13	41
K monel	0	0	0	C-28	163,400	132,400	22	45
	42	4.2×10^{20}	4.9×10^{19}	C-29	168,700	167,600	12	42
	84	6.1×10^{20}	7.6×10^{19}	C-26	167,600	166,500	11	43
Type 410 stainless steel	0	0	0	C-34	177,000	147,700	20	66
	42	1.1×10^{20}	1.1×10^{19}		194,200	171,200	17	64
	84	9.9×10^{20}	1.0×10^{20}		201,000	182,800	15	64
	126	2.4×10^{21}	2.9×10^{20}	C-34	204,700	188,900	15	58
	126	2.5×10^{21}	3.3×10^{20}	C-35	204,400	189,300	14	57

* All test data reported are averages of three samples tested. Reported by M. S. Robinson.[33]

10^{20} nvt at 40 to 50°C. No change in tensile properties was noted as a result of irradiation. It is concluded that annealing or irradiation damage in the magnesium alloys tested occurs below 40°C.

Churchman et al.[35] discuss the mechanism by which irradiation affects the strength of mild steel. They show that for a coarse- and fine-grained steel of the same compositions the effects of irradiation on yield and fracture stresses are about the same, both at room temperature and at liquid-nitrogen temperature. Maximum irradiation was 5.7×10^{19} nvt thermal. Fast flux was about 75 per cent of thermal. They conclude that irradiation hardening is caused by dispersed regions of radiation damage such as point defects that are sufficiently large to withstand thermally activated movements of dislocations. It appears that irradiation did not change the cohesive strengths of this mild steel.

Zakhorov and Maksimova[36] have reported on the effects of neutron irradiation on the martensite transformation. In this work steels with low (−10 to −39°C) M_s temperatures were used. Specimens of these steels were irradiated to a maximum dose of 10^{17} nvt. For different steels different effects were observed. In an 8 wt.% manganese–0.50 wt. % carbon steel, the M_s temperature was raised. In a 23 wt. % nickel–0.025 wt. % carbon steel, the M_s temperature was lowered. In all steels the effects of irradiation on the martensite transformation could be partially annealed out by storage at room temperature after irradiation for times ranging from 90 to 334 days. Holding at 100°C for 5 to 10 hr after irradiation practically eliminated the effects of irradiation in the 8 wt. % manganese–0.50 wt. % carbon steel. (D. C. Martin)

Selected Mechanical Properties of Cladding and Structural Materials

Zirconium and Zirconium Alloys

1. *Zircaloy-2.* Investigations at Hanford have shown that complete recrystallization of 25 per cent cold-worked Zircaloy-2 occurs between 100 and 1000 min at 600°C and between 10 and 100 min at 700°C. Grain coarsening was observed in 10 per cent cold-worked Zircaloy-2 after 100 min at 700°C and 1000 min at 600°C. Final grain size obtained in a given time and temperature was approximately 5 times greater after 10 per cent cold work than after 25 per cent.

Report of work at Auburn Research Foundation[37] gives values of 0.2 per cent yield strengths obtained for Zircaloy-2 from 47,000 psi in tension at room temperature to 12,900 psi at 800°F and modulus of elasticity values from 14.2×10^6 psi at room temperature to 6.8×10^6 psi at 800°F. This is in agreement with work at Battelle[38] where the 0.2 per cent offset yield strength was reported as 43,000 psi at room temperature and 16,200 psi at 800°F.

The creep strengths of annealed and 15 per cent cold-worked Zircaloy-2 are being investigated at Battelle[16,39,40] over a temperature range from 300 to 650°F. Comparison of two different lots of Zircaloy-2, in creep, has indicated that total creep deformations may vary by a factor of 2 from lot to lot of material tested at comparable stresses. The minimum creep rates obtained in 2000 hr, however, are not subject to such variance. The creep strength of 15 per cent cold-worked Zircaloy-2 is approximately twice that of the annealed material at comparable temperatures.

An investigation of burst strength of seamless and welded Zircaloy-2 annealed and in the cold-worked condition has shown the strengths of the welded tubes to be generally higher.[39] This is based on data from tests conducted on tubes of comparable diameters, wall thickness, heat-treated conditions, and test temperatures. The same general results have been observed for zirconium tubes. It has been found at Hanford that 1.5- by 0.060-in. zirconium and Zircaloy-2 tubing can be cold-formed (90 deg bend) in the annealed and cold-worked conditions with nominal thinning of the wall.

2. *Zircaloy-3.* Hanford reports complete recrystallization of 25 per cent cold-worked Zircaloy-3 between 100 and 1000 min at 600°C and between 10 and 100 min at 700°C. Specific times were shorter for complete recrystallization of Zircaloy-3 than for Zircaloy-2. Increasing hardness, apparently a result of gas contamination, was noted after annealing at 700 and 800°C in both helium and air. A second-phase grain-boundary precipitate was evident in the 10 and 25 per cent cold-worked material after 100 and 1000 min at 800°C.

The tensile properties of Zircaloy-3 at room temperature have been investigated at Knolls.[41]

Large differences were observed in strength properties between longitudinal and transverse directions of the rolled sheet. The thicker sheet, 0.185 in., was reported to have higher strengths than the 0.065-in.-thick sheet. Table IV-2 summarizes these data.

The results of strain-fatigue tests on Zircaloy-2 and -3 are represented graphically in Fig. 9. The creep properties of Zircaloy-3 determined at 300°F and reported by Battelle[39] show Zircaloy-3 to have less creep resistance than Zircaloy-2.

Table IV-2 TENSILE PROPERTIES OF ZIRCALOY-3 AT ROOM TEMPERATURE (KNOLLS DATA[41])

Mechanical properties	Perpendicular to rolling direction				Parallel to rolling direction			
(1)	(2)	(3)	(4)	(5)	(6)	(7)	(8)	(9)
	0.065-in. sheet							
Tensile strength, 1000 psi	62.7	3.61	71.5	31	60.0	2.23	66.9	14
			53.5				53.1	
0.2% offset yield strength, 1000 psi			63.8				33.8	
	53.1	4.16	42.4	29	28.0	1.82	22.5	13
Elongation in 1 in., %			38.5				32.6	
	34.8	1.46	3.17	30	28.7	1.21	25.2	14
Reduction of area, %			52.4				45.7	
	52.3	1.98	47.2	31	38.0	2.50	30.3	14
	0.185-in. sheet							
Tensile strength, 1000 psi			90.9				78.1	
	79.8	2.97	68.7	8	72.6	1.47	67.1	8
0.2% offset yield strength, 1000 psi			87.4				53.2	
	73.4	3.49	59.1	7	45.3	2.11	37.4	8
Elongation in 1 in., %			51.0				35.9	
	36.3	3.94	21.6	8	31.2	1.25	26.5	8
Reduction of area, %			57.2				47.4	
	50.7	1.74	44.2	8	42.0	1.44	36.6	8

Note: Columns 2 and 6, arithmetical average; 3 and 7, standard deviation; 4 and 8, 95 per cent probability that 95 per cent of values will be in this range; 5 and 9, number of tests.

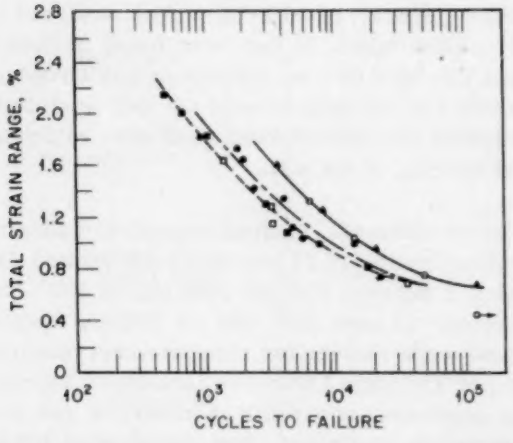

Fig. 9—Total strain range vs. cycles to failure for Zircaloy-2 and -3. ○, Zircaloy-3 at RT, large specimen (diam. = 0.187 in.). □, Zircaloy-3 at 550°F, large specimen (diam. = 0.187 in.). ▲, Zircaloy-2 at RT, large specimen (diam. = 0.187 in.). ●, Zircaloy-2 at RT, small specimen (diam. = 0.140 in.). ■, Zircaloy-2 at 550°F, small specimen (diam. = 0.140 in.).

Other Materials

Constant-temperature cyclic-strain-fatigue tests are reported by Knolls[42] for AISI 347 stainless steel. Results are interpreted in terms of plastic strain range–cycles-to-failure relation, $N^{1/2}\ \Delta\epsilon_p = C$, where N is the number cycles to failure, $\Delta\epsilon_p$ is the plastic strain range, and C is a constant. When considering the above relation, neither grain size nor anisotropy appears to have a significant effect. However, it does appear that the temperature parameter has a pronounced effect on the constant C which was not revealed for fracture ductility. The results are given in Table IV-3.

The creep strength of Inconel in fused salt has been investigated by Oak Ridge[43] in the 1300 to 1600°F temperature range in various environments. The effect of grain size on the creep properties depends on the testing temperature. At 1300°F the fine-grained material

is stronger than the coarse-grained material in all environments. At 1500°F the fine-grained material in argon and sodium is stronger but is weaker in fused salt. At 1650°F the fine-grained Inconel is weaker than coarse-grained Inconel in all environments. Corrosion induced by the fused salt causes a reduction in the creep and rupture properties of Inconel at all temperatures. This reduction is more marked at the higher temperatures and for test-section thicknesses for less than 0.06 in. It was also found that the rupture life of Inconel was not decreased by testing under a biaxial stress system but that the total elongation at failure in the direction of the maximum stress may be substantially reduced. By subjecting tubes to various ratios of axial and tangential stresses and measuring the resultant creep rates, a considerable change in rupture life was observed. The rupture life varied from 200 to 2000 hr with significant variations in creep rates noted.

Table IV-3 FATIGUE PROPERTIES OF AISI TYPE STAINLESS STEEL (KNOLLS DATA[42])

Temp., °C	Strain range, 10^{-3} in.	Cycles to failure	Stress range, 1000 psi
RT	15	4×10^3	120
RT	5	2×10^5	62
200	19	3.5×10^3	96
200	4	2×10^5	58
350	19	3.5×10^3	90
350	4	1.5×10^5	62
500	20	1×10^3	92
500	4	1×10^5	62
600	19	1×10^3	84
600	7	1.5×10^4	60

Table IV-4 MECHANICAL PROPERTIES OF NIOBIUM AND NIOBIUM ALLOYS*

Composition (balance niobium), wt.%	Hardness, VHN	Ultimate tensile strength, psi	Elongation, %
100 Niobium†	87	36,700	29.3
0.371 Oxygen	314	122,000	10.4
0.565 Oxygen	390	Cracked	
7.5 Molybdenum	159	90,000	13
7.5 Tungsten	113	75,500	10

* Data reported by Jepson.[2]

† Impurities 0.022 wt.% oxygen, 0.006 wt.% nitrogen, 0.001 wt.% hydrogen.

Recent British work[44] on niobium alloys has shown that oxygen increases the strength but decreases ductility (Table IV-4). Initial work on alloys showed that molybdenum and tungsten produce moderate strengthening. Much work remains to be done on mechanical properties of niobium alloys, especially those which have good oxidation resistance.

Oak Ridge[44] work on the annealing behavior of niobium has shown that recovery begins at 800°C, but recrystallization is not complete until 1100°C for heavily reduced and 1350°C for lightly reduced niobium. Arc-cast niobium had larger recrystallized grain size than powder-metallurgy niobium. (F. R. Shober)

References

1. Oak Ridge National Laboratory, Dec. 13, 1957. (Unpublished.)
2. M. D. Jepson, The Metallurgy of Niobium, *Research*, 10: 10 (October 1957).
3. R. W. Dayton and C. R. Tipton, Jr., Progress Relating to Civilian Applications During August 1957, BMI-1220, Sept. 1, 1957. (Confidential AEC report.)
4. J. G. Gratton, Solubility of Carbon in Sodium at Elevated Temperatures, KAPL-1807, June 30, 1957. (Unclassified AEC report.)
5. E. G. Brush, The Behavior of Alumel, of Chromel, and of Uranium-Zirconium Alloys in Heavy Liquid Metals, KAPL-M-EGB-25, May 21, 1957. (Confidential AEC report.)
6. E. E. Hoffman and D. H. Jansen, Lithium Symposium — Analytical Procedures and High-temperature Corrosion. Reading List, CF-57-10-6, Oct. 1, 1957. (Unclassified AEC report.)
7. W. E. Bost, Technical Information Service Extension, August 1957. (Unpublished.)
8. Pressurized Water Reactor Project, Technical Progress Report, WAPD-MRP-70, Oct. 23, 1957. (Unclassified AEC report.)
9. J. G. Goodwin and E. L. Richards, "Progress in the Resolution of Anomalous Zirconium Alloy Corrosion Problems," in the Bettis Technical Review, Vol. I, No. 2, Reactor Metallurgy, WAPD-BT-2, July 1957. (Unclassified AEC report.)
10. B. Lustman, Zirconium-Water Reaction Data and Application to PWR Loss-of-Coolant Accident, WAPD-SC-543, May 1957. (Unclassified AEC report.)
11. J. A. Burka, C. S. Crause, and R. E. Swift, Scaling of Zirconium and Zirconium Alloys, Technical Progress Report No. 1, AECU-3561, August 1957. (Unclassified AEC report.)
12. V. H. Troutner and R. L. Dillon, Observations on the Mechanisms and Kinetics of Aqueous Aluminum Corrosion, HW-51849, Sept. 30, 1957. (Unclassified AEC report.)

13. F. H. Krenz, Corrosion of Aluminum-Nickel Type Alloys in High-temperature Aqueous Service, *Corrosion*, 13: 575-581 (September 1957).
14. I. Cohen, Corrosion of Experimental Aluminum Alloys in High-temperature Water — Report No. 9, WAPD-PWR-PMM-1247, Aug. 22, 1957. (Unclassified AEC report.)
15. R. J. Beaver, R. C. Waugh, C. F. Leitten, Jr., and W. R. Burt, Jr., Investigation of the Factors Affecting Sensitization of Army Package Power Reactor (APPR-1) Fuel Elements, ORNL-2312, Oct. 8, 1957. (Unclassified AEC report.)
16. W. D. Klopp, C. T. Sims, and R. I. Jaffee, Oxidation-resistant Niobium Alloys, BMI-1238, Dec. 1, 1957, pp. 35-40. (Unclassified AEC report.)
17. D. V. Doane, Oxidation-resistant Coatings for Molybdenum, WADC-TR-54-492 (Pt. 3), April 1957. (Unclassified USAF report.)
18. R. Frank, Properties of Molybdenum Turbine Buckets, Regional High-temperature Materials Conference, Cleveland, Ohio, April 1957.
19. V. A. Parfenov, Reasons for the Intergranular Cracking of the Surface of Articles in EI-437 Alloy, *Metallovedenie i Obrabotka Metallov*, 1: 36-40 (1955); *Metallurgical Abstracts*, 25: 86 (1957).
20. F. Malamand and G. Vidal, Effect of Oxidation on the Surface Composition of Heat-resistant Alloys, *Recherche aéronautique*, 56: 47-57 (1957).
21. National Bureau of Standards, 1957. (Unpublished.)
22. National Bureau of Standards, October 1957. (Unpublished.)
23. J. J. Trillat, L. Testian, and C. Lecomte, Electron Diffraction Study of Nitriding of Nickel, *Comptes rendus*, 244(5): 596-598 (1957).
24. Semiannual Summary Research Report in Metallurgy for July–December 1956, ISC-835, Aug. 23, 1957. (Unclassified AEC report.)
25. R. W. Vook, Expansion of Copper upon Low-temperature Deuteron Irradiation, University of Illinois Report No. 6, September 1957. (University of Illinois, Urbana, Ill.)
26. G. C. Magnuson, W. Palmer, and J. S. Koehler, Isothermal Annealing Below 60°K of Deuteron Irradiated Noble Metals, University of Illinois Report No. 5, 1957. (University of Illinois, Urbana, Ill.)
27. A. W. Overhauser, Stored Energy Measurements in Irradiated Copper, *Physical Review*, 94: 1551 (1957).
28. B. T. M. Willis and R. E. Smallman, An X-ray Study of Neutron Irradiated LiF, *The Philosophical Magazine*, 2: 1018 (1957).
29. I. Binder and W. J. Sturm, Equivalence of X-ray Lattice Parameter and Density Changes in Neutron-irradiated LiF, *Physical Review*, 96: 1519 (1954).
30. D. T. Keating, X-ray Measurement of Pile-irradiated LiF, *Physical Review*, 97: 832 (1955).
31. F. W. Albaugh, Plutonium Recycle Program Monthly Report for August 1957, HW-52303 A2, Sept. 10, 1957. (Unclassified AEC report.)
32. R. S. Kemper and D. L. Zimmerman, Neutron Irradiation Effects on the Tensile Properties of Zircaloy-2, HW-52323, Aug. 22, 1957. (Unclassified AEC report.)
33. M. S. Robinson, Radiation Damage Studies Program, ETR Loop Materials Progress Report II, IDO-16409, Sept. 16, 1957. (Unclassified AEC report.)
34. M. J. Makin and F. J. Minter, Mechanical Properties of Irradiated Magnesium Alloys, AERE-M/M-174, July 1957. (Unclassified British report.)
35. A. T. Churchman, I. Mogford, and A. H. Cottrell, The Hardening and Embrittlement of Steel by Irradiation with Neutrons, *The Philosophical Magazine*, 2(22): 1271-1275 (October 1957).
36. A. I. Zakhorov, and O. P. Maksimova, Effect of Neutron Irradiation on Martensitic Transformation, *Doklady Akademii Nauk*, 114(6): 1195-1198 (June 1957).
37. R. E. Morris, Tests of Special Materials, Final Report, AECU-3477, Mar. 20, 1957. (Unclassified AEC report.)
38. F. R. Shober, J. A. VanEcho, L. L. Marsh, and J. R. Keeler, The Mechanical Properties of Zirconium and Zircaloy-2, BMI-1168, Feb. 18, 1957. (Unclassified AEC report.)
39. R. W. Dayton and C. R. Tipton, Jr., Progress Relating to Civilian Applications During September 1957, BMI-1226, Oct. 1, 1957. (Unclassified AEC report.)
40. R. W. Dayton and C. R. Tipton, Jr., Progress Relating to Civilian Applications During October 1957, BMI-1232, Nov. 1, 1957. (Unclassified AEC report.)
41. R. L. Mehan, Tensile Properties and Metallographic Study of Zircaloy-3 Strip, KAPL-M-RLM-12, June 13, 1957. (Unclassified AEC report.)
42. E. E. Baldwin, G. J. Sokol, and L. F. Coffin, Cyclic Strain Fatigue Studies on AISI Type 347 Stainless Steel, KAPL-M-EEB-16, Apr. 19, 1957. (Unclassified AEC report.)
43. J. R. Wein, Jr., D. A. Douglas, and W. D. Manly, Oak Ridge National Laboratory, June 18, 1957. (Unpublished.)
44. J. P. Page, The Annealing Behavior of Cold-rolled Niobium, ORNL-2372, Oct. 1, 1957. (Unclassified AEC report.)
45. R. S. Kemper and W. S. Kelly, Effects of Irradiation on the Mechanical Properties of Zirconium, Proceedings of the American Society for Testing Materials, 1956 (Preprint No. 78).
46. D. E. Johnson, Additional Observations on the Flow Stress Recovery of Zircaloy-2, HW-50340, June 6, 1957. (Unclassified AEC report.)
47. Arc-Cast Molybdenum and Its Alloys, Climax Molybdenum Co., New York, 1955.

Melting

Research and development studies relating to the melting and casting of fuel materials continue to be concentrated in areas relating to metal quality and alloy homogeneity. Unalloyed uranium has received a considerable portion of this effort.

In this regard National Lead Co. has reported efforts toward the production of unalloyed uranium fuel slugs by centrifugal casting.[1] The slugs are sound, as indicated by the high densities consistently exhibited. The successful blending of various enrichments of unalloyed uranium was also reported. Material whose U^{235} content ranged from normal to 2.779 wt. % was blended and, from isotopic analyses, was determined to be within 0.01 wt. % of the desired 1.25 wt. % U^{235}.

The factors affecting the hydrogen content of dingot uranium are being studied at Battelle.[2] The stated objective of this study is to determine the kinetic behavior of hydrogen in the thermite reaction as it is related to the water content of bomb charges. The permeation of the slag (MgF_2) by hydrogen, the viscosity of the slag, and the effect of minor constituents on the viscosity are specific subjects being investigated. Considerable experimental difficulties are being experienced because of the corrosive nature of the molten slag.

Further studies relating to unalloyed uranium are in progress. Efforts are continuing in the theoretical study of the variables involved in the solidification of uranium ingots. Results to date have established the validity of the method of analysis employed, and additional refinements in the mathematical model that describes the heat flow in the casting are in progress. Another study, an investigation into the chemical reactions which take place during the vacuum melting of uranium, has been initiated recently.[2] The role of impurities in these reactions is being studied by analyzing the melt and outgassing products.

The quality of Zircaloy has been of interest to several fuel-element fabricators. Zircaloy has been examined from several viewpoints, and evaluations of various materials have indicated there is some lack in quality control from melting practice to primary fabrication. Argonne has commented on the losses caused by the poor quality of Zircaloy-2 ingots.[3] A 5 to 10 per cent loss was attributed to porosity, tungsten inclusions, and laps and seams present in the ingots. Bettis reports the continuing difficulties caused by stringers that become evident during the corrosion screening of cladding material. No identification was made of the materials responsible for the stringers and no success was achieved, with commercial treatments, in salvaging material that exhibited this poor corrosion resistance. However, vacuum arc-melting techniques were found to minimize or eliminate stringering, and a major portion of production melting is now done by the vacuum consumable-electrode arc-melting process.

Hot and Cold Working

Fabrication studies performed at Battelle[2] show that a uranium–20 wt. % niobium alloy is fabricable at room temperature and at 1500 and 1700°F in a titanium jacket. An 80 wt. % niobium alloy broke up under similar conditions.

An examination by Knolls of Zircaloy forged from 12-in.-diameter ingots to $2\frac{5}{8}$- to $3\frac{5}{8}$-in.-diameter rods determined that several types of defects were present.[4] Of the rods examined over a 4-month period, 77 per cent were free of defects. The four typical defects were (1) surface cracks and cold shuts too deep to be removed by normal machining cleanup, (2) internal radial cracks, (3) center bursting, and (4) center porosity. Although ingot shrink pipe caused a portion of the internal defects, center burst and radial cracking could be related to faulty forging practices aggravated to some extent by the columnar-grained ingot. The study indicates that close forging control is necessary

and that extrusion fabrication procedures would improve the over-all quality of the rods.

(E. L. Foster, Jr.)

Cladding

Roll Cladding

Methods of eliminating "dog boning" and of improving surface finish of roll-clad fuel plates have been investigated.

"Recessed cover plates" were used in the processing of fuel plates. Examination of the fuel plates by nondestructive tests revealed that dog boning in Zircaloy-clad uranium-zirconium fuel plates had been eliminated with the use of this type of cover plate. It was necessary to weld the core to the Zircaloy-2 "picture frame" to eliminate dog boning of core ends in the picture frame type of fuel elements.

Improved fuel-plate surface properties and improved dimensional uniformity were obtained when thicker protective carbon-steel outer packs were used to process fuel elements for the Experimental Boiling Water Reactor (EBWR).

(E. S. Hodge)

Pressure Bonding

The French[5] are investigating the use of a hydrostatic bonding technique for the cladding of fuel elements. Uranium slugs are clad with magnesium by use of an oil pressure of 40 kg/cm^2 at 752°F. The thermal expansion of magnesium is about twice that of uranium; consequently, after pressing, the magnesium remains in contact with the uranium at lower temperatures.

Several laboratories are investigating pressure-bonding techniques for the preparation of Zircaloy-clad flat-plate uranium dioxide fuel elements. In the work at Battelle,[2,6,7] bonding is achieved by the use of a helium gas pressure of 10,000 psi at a temperature of 1550°F. The components to be bonded are cleaned, assembled, sealed in an evacuated envelope, and pressure bonded. The surface condition of the Zircaloy has a pronounced influence on the resultant quality of the bond. Optimum bonding is achieved with either hot-rolled or annealed Zircaloy which is surface finished by machining or by a grit-belt-abrasion process. The bonds exhibit complete grain growth across the interface and almost no contamination along the original bond interface.

A combination brazing and gas pressure-bonding technique is being investigated by Bettis[8] for the preparation of flat-plate uranium dioxide fuel elements. The Zircaloy components are plated with nickel by a chemical replacement technique. They are then assembled, sealed by fusion edge welding, and subjected to 60 psi of helium gas at a temperature of 1850°F, which is above the nickel-zirconium eutectic temperature.

Knolls has also been investigating techniques for the cladding of compartmented flat-plate uranium dioxide fuel elements. Cursory pressure-bonding studies have been conducted in vacuum at elevated temperatures using a static load to apply pressure. A sandwich type specimen consisting of two Zircaloy plates was bonded at 825°C for 20 hr with a pressure of 1000 psi. An excellent bond was obtained with complete grain growth across the original interface. A three-plate fuel assembly incorporating Al_2O_3–15 vol. % UO_2 fuel was also bonded under a pressure of 2000 psi at 825°C for 20 hr. Metallographic examination revealed grain growth across 80 per cent of the bond interface. No mention was made of the prior heat-treatment or surface-conditioning treatment employed for the Zircaloy.

A gas pressure-bonding technique is being utilized by Battelle for the bonding and cladding of zirconium subassemblies in a one-step operation. A subscale 2- by 2- by 6-in. subassembly has been bonded in 5 hr at 1550°F using a helium gas pressure of 10,000 psi. The clad and core components were assembled in a light stainless-steel can which was evacuated and sealed. Excellent dimensional control was achieved without the use of external jigging. Bonding was influenced by the heat-treatment and surface condition of the Zircaloy, as in the studies involving the Zircaloy cladding of uranium dioxide fuel elements.

Several studies are being conducted to obtain a better understanding of the bonding process. Results from these studies are especially applicable to the pressure-bonding processes. The effect of pressure on the kinetics of diffusion occurring at the interface between two dissimilar metals is being investigated by Sylvania.[9,10] Previous work has shown the influence of pressure on an aluminum-nickel diffusion couple. Growth at the interface was retarded, and the formation of the Ni_2Al_3 phase was suppressed with an increase in pressure.

Current investigations are concerned with the diffusion kinetics of the aluminum-uranium systems. Several diffusion couples have been heat-treated in a temperature range from 520 to 570°C under a pressure of 1¼ and 5 tsi. Results of these tests are presented in Table V-1.

Table V-1 THICKNESS OF UAl_3 LAYER FORMED AT ALUMINUM-URANIUM INTERFACE UNDER VARIOUS CONDITIONS OF TEMPERATURE, TIME, AND PRESSURE (SYLVANIA DATA[18])

Temp., °C	Pressure, tsi	Time, hr	Av. thickness of UAl_3 layer, mm	Standard deviation, mm
520	5	8	2.365	±0.022
520	5	16	3.426	±0.052
520	5	24	4.218	±0.028
520	1¼	24	2.552	±0.351
560	5	16	4.148	±0.037
560	5	24	5.027	±0.064
560	5	29	5.577	±0.120
570	5	8	3.146	±0.029
570	5	16	4.418	±0.045
570	1¼	24	4.284	±0.130

An increase in pressure resulted in greater growth at the interface. This is contrary to the results obtained for the aluminum-nickel system but is in agreement with results reported by LeClaire and Bear.[11] It is significant that a common relation does not exist between pressure and the kinetics of diffusion for all systems.

Battelle[6,7] is conducting a study of bonding fundamentals. This study utilizes a simulated single asperity consisting of a gold needle with a hemispherical point brought into contact with a flat gold plate. The degree of bonding is measured by a normal force to rupture the bond or by electrical-resistivity measurements. The bond strength has been found to increase in proportion to the applied load. It is postulated that the bond can be separated into the following areas: (1) area formed instantly through adhesion under applied load, (2) area formed by diffusion, and (3) area formed from effects of creep if the load is maintained. (S. J. Paprocki)

Vapor Deposited Coatings

As part of an effort to obtain high-temperature oxidation-resistant coatings on molybdenum, tungsten, and tantalum, work at Georgia Institute of Technology[12] explored vacuum evaporation and sputtering of aluminum, silicon, nickel, and rhodium on a molybdenum substrate. To obtain thicker coatings, equipment was designed and operated in which powdered metals were entrained in a gas stream, blown through an electric arc, and impinged on the surface to be coated. This met with only limited success. Exploratory work was also done on the siliconizing of molybdenum by the hydrogen reduction of silicon tetrachloride, a technique reported extensively by a number of others. The molybdenum disilicide coatings protected the molybdenum from oxidation at 1500°F so long as no gross imperfections existed. The above methods were abandoned in favor of flame spraying of ceramic powders.

(J. M. Blocher, Jr.)

Welding and Brazing

Work of general interest on welding reactor core materials has been published recently. Workers at Harwell[13] experimented with inert-gas-shielded tungsten-arc welding, projection welding, and upset butt welding for the fabrication of unbonded Zircaloy-2–clad fuel elements with metallic cores. As had been found in previous work in this country, they observed that weld area contamination with oxygen and nitrogen rendered the Zircaloy more susceptible to aqueous corrosion. The method selected for production welding was the tungsten-arc process, carried out in a vacuum-purged dry box.

Studies of the welding of uranium at Aldermaston[14] and Los Alamos[15] have also been published. Satisfactory welds were obtained by inert-gas-shielded tungsten-arc welding and resistance spot welding. No evidence of any tendency for uranium to crack during welding because of hot shortness was observed using the Houldcroft crack-sensitivity test.

(R. E. Monroe)

Nondestructive Testing

A bibliography of reports on flaw detection by radiographic, ultrasonic, eddy-current, and "frost-test" methods has been prepared by Lanier.[16] A compilation by Smith and Scott[17] includes, in addition to the above, literature on penetrant, leak testing, and electromagnetic techniques and information on the availability of the reports. There are not many duplications in these two bibliographies.

Two recent review articles by McGonnagle[18,19] discuss the techniques and limitations (quantitative values for sensitivity in several instances) of the most widely used nondestructive testing techniques. It is pointed out[18] that the frost test as normally employed (clad specimen coated with acenaphthene and passed through an induction heater) may not reveal partially bonded areas or areas having a minimum dimension of less than ½ cm. Temperature-sensitive phosphor coatings are more discriminative but require observation under ultraviolet light while in the transient-temperature state.

Many applications and techniques for ultrasonic inspection of materials and finished elements are reported. Stedronsky[20] of Du Pont describes in detail an automatic scanning mechanism for nonbond detection of ribbed tubular elements. The electronic circuit had been described previously by Hanford.[21] The possibilities (geometrical) for transmission inspection of hollow cylinders have also been discussed.[22] A probe located inside the cylinder would have many advantages but presents design problems for production scanning devices. It is also reported[23] that pulse-reflection techniques will detect seams and striations 1 to 2 mils deep and ⅛ in. long and subsurface voids up to 6 mils beneath the surface of uranium slugs. However, the instrument is not sensitive to dents or inclusions. Bettis has found that immersed ultrasonic transmission will locate 95 per cent of all core-cladding unbonded areas 1/16 in. in diameter or larger.

Argonne[24] reports the successful bond testing of 8 EBWR fuel plates, after they had been welded into a subassembly, with the use of a specially built two-arm probe. The development work on an ultrasonic "fluoroscopy" unit in which 4-in.-square crystals will be used is mentioned. One crystal consists of a mosaic of 196 segments, each of which can be excited independently. By combining this with a video sweep of 30 frames per second and z-axis modulation, a visual image of the test object can be obtained.

One of the difficult problems in the development of nondestructive inspection techniques is determining the sensitivity of any new instrument to the various sizes and types of flaws that need detection. There are several approaches to this problem. Battelle has used mercury-tank models to establish optimum probe geometry and sensitivity (under ideal conditions) of the electrical-potential method of tie-bar weld inspection. As a final evaluation of the technique, a statistical correlation of inspection results with destructive examination of a large number of production welds is planned.[7] Hanford reports that the final determination of rejection limits of the redesigned frost-test apparatus for bond inspection of ⅝-in.-diameter Zircaloy-clad elements must await fabrication of elements for inspection and destructive examination. Sylvania-Corning[10] is having difficulty fabricating sample fuel plates with intentional flaws for calibration of ultrasonic bond-testing equipment. Knolls[25] has coextruded 35 fuel elements containing tungsten and oxide inclusions in the core; seam laps, folds, pits, and unsized areas; and scratches and copper stringers in cladding. These are to be used by Metals and Controls and Olin-Mathieson to calibrate their ultrasonic and eddy-current equipment. (W. H. Goldthwaite)

References

1. John W. Simmons, editor, Summary Technical Report for the Period July 1, 1957, to Sept. 30, 1957, NLCO-690, October 1957. (Confidential AEC report.)
2. R. W. Dayton and C. R. Tipton, Jr., Progress Relating to Civilian Applications During November 1957, BMI-1238, Dec. 1, 1957. (Unclassified AEC report.)
3. R. E. Macherey, C. H. Bean, N. J. Carson, Jr., and J. R. Lindgren, Manufacture of Fuel Plates for EBWR, ANL-5629, June 1957. (Unclassified AEC report.)
4. R. F. Lupi, Macroscopic Examination of Zircaloy-3A and Zircaloy-2 Primary Extrusion Billet Material, KAPL-M-RFL-8, May 3, 1957. (Unclassified AEC report.)
5. M. Gauthron, Thermopneumatic Cladding, Fuel Elements Conference, Paris, Nov. 18–23, 1957, TID-7546, Book 1. (Unclassified AEC report.)
6. R. W. Dayton and C. R. Tipton, Jr., Progress Relating to Civilian Applications During September 1957, BMI-1226, Oct. 1, 1957. (Unclassified AEC report.)
7. R. W. Dayton and C. R. Tipton, Jr., Progress Relating to Civilian Applications During October 1957, BMI-1232, Nov. 1, 1957. (Unclassified AEC report.)
8. Westinghouse Atomic Power Division, Dec. 20, 1957. (Unpublished.)
9. L. W. Kates, Technical Progress Report for the Period July 1 to Aug. 31, 1957, SCNC-254, Dec. 15, 1957. (Secret AEC report.)

10. L. W. Kates, Monthly Technical Progress Report for the Period Ending Sept. 30, 1957, SCNC-256, Dec. 15, 1957. (Secret AEC report.)
11. A. D. LeClaire and I. G. Bear, The Interdiffusion of Uranium and Aluminum, *Journal of Nuclear Energy*, 2: 229-242 (1956).
12. J. D. Walton, R. B. Belser, and N. F. Ponlos, Investigation of High-temperature-resistant Materials, Quarterly Report Nos. 1 through 8, Mar. 15, 1955 to Mar. 15, 1957. (Available from Engineering Experiment Station, Georgia Institute of Technology, Atlanta, Ga.)
13. J. G. Purchas, D. R. Harris, and H. Cobb, The Welding of Zircaloy-2, *British Welding Journal*, 42(9): 412-421 (September 1957).
14. J. R. C. Gough and D. Roberts, The Welding of Uranium, *British Welding Journal*, 42(9): 393-403 (September 1957).
15. Los Alamos Team Favors TIG for Titanium Welds, *Welding Engineer*, 42(12): 72 (December 1957).
16. Sidney F. Lanier, Technical Information Service Extension, July 1957. (Unpublished.)
17. R. J. Smith and T. W. Scott, comp., Nondestructive Testing, A Literature Search, TID-3521, November 1957. (Unclassified AEC report.)
18. W. J. McGonnagle, Nondestructive Testing of Reactor Fuel Elements, *Nuclear Science and Engineering*, 2: 602-616 (September 1957).
19. W. J. McGonnagle, Nondestructive Testing of Reactor Components, *Nucleonics*, 15(10): 78-81 (October 1957).
20. V. E. Stedronsky, Nonbond Detector for Ribbed Tubes, DP-240, September 1957. (Confidential AEC report.)
21. R. W. Leep and J. D. Ross, A Simplified Electronic Circuit for Ultrasonic Inspection, DP-120, January 1956. (Unclassified AEC report.)
22. C. L. Frederick, Evaluation of Ultrasonic Attenuation Techniques for Testing Hollow Uranium Cores for Transformation, HW-48875, Mar. 5, 1957. (Confidential AEC report.)
23. C. E. Fitch, Jr., Ultrasonic Detection of Surface Defects in Uranium, HW-51979, Sept. 3, 1957. (Unclassified AEC report.)
24. Metallurgy Division Quarterly Report for October, November, and December, 1956, ANL-5709, Dec. 31, 1956. (Confidential AEC report.)
25. R. F. Lupi and C. M. Olds, Fabrication of Defective Fuel Elements as Standards for the Calibration of Nondestructive Test Equipment, KAPL-M-RFL-9, July 5, 1957. (Unclassified AEC report.)

LEGAL NOTICE

This document was prepared under the sponsorship of the U. S. Atomic Energy Commission. Neither the United States, nor the Commission, nor any person acting on behalf of the Commission:

A. Makes any warranty or representation, express or implied, with respect to the accuracy, completeness, or usefulness of the information contained in this document, or that the use of any information, apparatus, method, or process disclosed in this document may not infringe privately owned rights; or

B. Assumes any liabilities with respect to the use of, or for damages resulting from the use of any information, apparatus, method, or process disclosed in this document.

As used in the above, "person acting on behalf of the Commission" includes any employee or contractor of the Commission to the extent that such employee or contractor prepares, handles or distributes, or provides access to, any information pursuant to his employment or contract with the Commission.